

TEXT and rectangles in blue will NOT show on printed copy

Type final title of thesis or dissertation (M.S. and Ph.D.) below . If your title has changed since your submitted an Application for Graduate Degree, notify Graduate Office.

Presented to
the faculty of the School of Engineering and Applied Science
University of Virginia

in partial fulfillment
of the requirements for the degree

by

Name

Month degree is awarded

Year

APPROVAL SHEET

is submitted in partial fulfillment of the requirements

for the degree of

Stephen M. Cronk
AUTHOR *signature*

Please insert committee member names below:

Advisor

Accepted for the School of Engineering and Applied Science:

Dean, School of Engineering and Applied Science

Month degree is awarded

Year

Acknowledgements

A huge thanks to Shayn, Dr. Yates, Dr. Herman, and my committee as a whole for their unwavering support, guidance, and advice. I also want to thank everyone in the Peirce and Yates labs for showing me the ropes during the first few months, and always being there to help when a tube explodes in the centrifuge, or the precious stem cells are sucked down the drain. I could never ask for a better group of people to be in grad school with.

Abstract

Diabetic retinopathy is a debilitating disease that leads to progressive retinal vascular pathologies and ultimately to vision loss which current treatments are unable to reverse. We have recently shown that intra-vitreous injection of adipose-derived stem cells (ASCs) stabilize retinal microvasculature and encourage regeneration of damaged capillary beds in several mouse models of retinal vasculopathy. ASCs are advantageous because of their relative ease of harvest from accessible fat depots, as well as their potential for autologous or allogeneic treatment. Understanding the status of ASCs harvested from diabetic patients is of critical importance for moving forward with autologous therapies. Using the hyperglycemic Akimba mouse model of diabetic retinopathy, we probed the differences in treatment efficacy and function of mouse adipose-derived stem cells (mASCs) derived from healthy vs. diabetic Akimba mice. Akimba mice received intra-vitreous injections of Dil-labeled mASCs, and retinæ were imaged four weeks later by confocal microscopy. mASCs from healthy, non-diabetic mice were more effective than diabetic mASCs in protecting the diabetic retina from vascular dropout. mASC viability was assessed using TUNEL and EdU incorporation assays, which revealed that healthy mASCs proliferate more rapidly and undergo less apoptosis than diabetic mASCs. Finally, when compared to diabetic mASCs, healthy mASCs secreted more angiogenesis-promoting factors as determined by high-throughput ELISA. Our findings suggest that injected ASCs derived from diabetic mice have a decreased ability to affect the retinal vasculature likely due to decreased cell viability and secretion of angiogenic factors, and support the utility of an allogeneic approach in the clinical arena.

Introduction

Stem cell therapy is a central tenet in regenerative medicine, and has far-reaching applications. Stem cell therapy is currently being investigated for over fifty diseases, including cardiovascular, lung, eye, and neurodegenerative disorders, as well as cancer and HIV/AIDS.¹ However, a limiting factor in both carrying out this research and applying it in the field is still the availability of stem cells.² Several types of stem cells exist, including embryonic stem cells (ESCs), bone marrow-derived stem cells (BMSCs), hematopoietic stem cells (HSCs), and adipose-derived stem cells (ASCs). While ESCs initially have the advantage of being totipotent and therefore able to regenerate any tissue, their use brings up considerable ethical concerns as harvesting ESCs destroys the embryo. BMSCs are the most thoroughly described stem cell population, but their isolation is a painful process, and obtaining a large enough quantity of BMSCs makes their widespread use impractical.³ The “ideal” stem cell for therapy is one that can be harvested in large quantities using a relatively painless procedure and manufactured using current Good Manufacturing Practice guidelines, can be reliably differentiated along multiple lineage pathways, and can be transplanted safely autogeneically or allogeneically.²

Adipose-derived Stem Cells

Recently, adipose-derived stem cells (ASCs) have come under greater focus as an attractive source of stem cells for therapy, as they are able to meet all of these conditions. ASCs are obtained from white adipose tissue, which is readily available due to the prevalence of obesity in the United States and abroad,⁴ and the resulting high numbers for liposuction procedures each year.⁵ Zuk et al. reported 2 to 6×10^8 cells from 300cc of lipoaspirate.⁶ Much like MSCs and BMSCs, ASCs were shown to be capable of differentiation towards adipogenic, osteogenic, chondrogenic, and myogenic lineages, by medium induction and confirmed by histology and immunohistochemistry.⁶ ASCs

derived from human adipose tissue have also been shown to be able to differentiate into pericytes, and this differentiation is likely controlled by local hypoxic and inflammatory conditions.⁷⁻⁹

The isolation of ASCs from adipose tissue was originally described by Rodbell and Jones in the 1960s,¹⁰ and aside from being optimized in various ways, remains very similar today. In short, the process begins by mechanically cutting the samples into small pieces, followed by a collagenase digestion at 37C. After passing the digested sample through a mesh filter, repeated centrifugation and wash steps yield the stromal vascular fraction (SVF), which contains the ASCs and other cell types such as erythrocytes, fibroblasts, pericytes, and endothelial cells.¹⁰ Finally, as the SVF is cultured on gel-coated slides, only the adherent ASCs are retained while the other cell types are eliminated with each media change and passage.³

Adipose tissue derives from the mesenchymal germ layer of the embryo, and it is of little surprise that ASCs are very similar to MSCs and are thought to be a source of MSCs.¹¹ These two cell types have been compared using multiple techniques, which demonstrate that they are similar, but distinct. ASCs and MSCs share more than 90% of their surface immunotype.⁶ In addition, MSCs and ASCs share a similar transcriptome. A study comparing their transcriptomes using Affymetrix chips found a 50% correlation between MSCs and ASCs, in contrast to 71% correlation between ASCs from different donors and 64% between MSCs from different donors.¹²

Applications of ASCs

The therapeutic potential of ASCs has been demonstrated with success in several regenerative applications (Figure 1). ASCs have been extensively studied for use in regenerating damaged tissue following myocardial infarction (MI). In one such study, suspended ASCs were transplanted into infarct border zones in a rat model of MI. Analysis of these regions 30 days post-injection revealed that treatment with rat ASCs

led to smaller infarct zones and higher left ventricular function.¹³ A similar study also in a rat MI model, but using human ASCs showed similar improvements after treatment, with the interesting result that ASCs persisted in peri-infarct region at the one-month analysis timepoint.¹⁴ When transplanted into rat livers with acetaminophen-induced damage, the leading cause of acute liver failure, ASCs facilitated regenerated liver tissue by enhancing hepatocyte regeneration while reducing local inflammation.¹⁵

Another prominent area of research into ASCs therapy, which we are particularly interested in, is in diabetes and diabetic complications. Multiple groups have been successful in the differentiation of ASCs into insulin-producing cells using a succession of differentiation media, an important step towards treating type 1 diabetes by replacing destroyed pancreatic beta cells.^{16–18} ASCs have been shown to improve diabetic wound healing,¹⁹ neuropathy,²⁰ and nephropathy,²¹ among other complications associated with diabetes. Our group has recently shown that intra-vitreal injection of adipose-derived stem cells (ASCs) stabilizes the retinal microvasculature and encourages regeneration of damaged capillary beds in several mouse models of retinal vasculopathy, including the Akimba mouse model of diabetic retinopathy.²² Others have recently shown similar positive findings using the streptozotocin (STZ) mouse model of diabetic retinopathy.²³

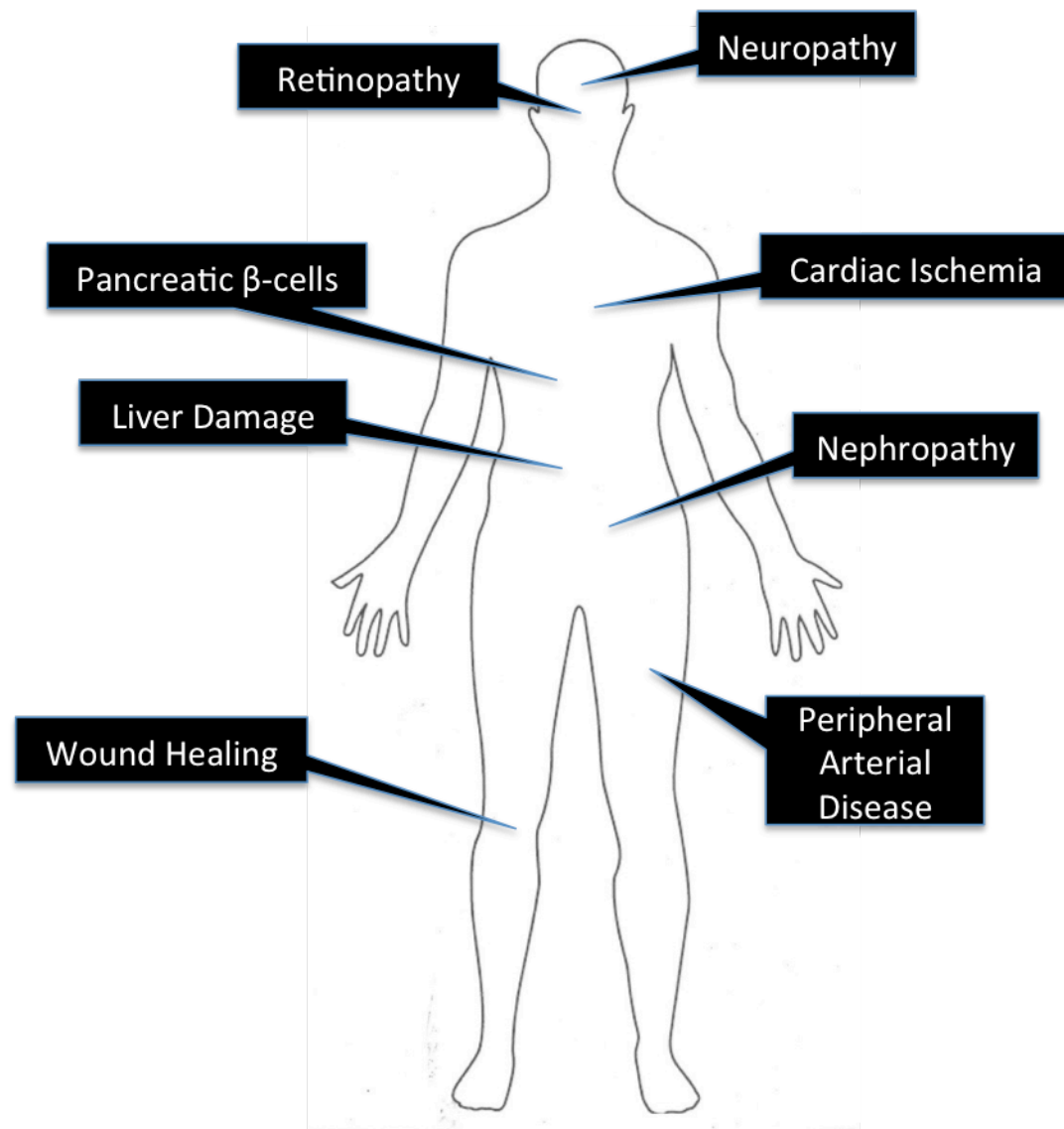


Figure 1: Major areas of research in ASC therapy. Image adapted from en.wikipedia.org.

Putative mechanisms underlying the ability of ASCs to modulate the vasculature

The precise mechanism for ASC-mediated modulation of the microvasculature is still under investigation, but there is support for several hypotheses (Figure 2). The ability of ASCs to differentiate down multiple lineages and self-renew lends itself to their use as replacements for lost or damaged cells. ASCs also secrete a wide array of pro-survival and angiogenic factors, which led to the hypothesis that they exert their regenerative effects through a paracrine mechanism. These two hypotheses have recently been tested head-to-head in a model of MI, where both ASCs and ASC-conditioned media were injected into peri-infarct regions in a mouse model of MI, and infarct size and cardiac function assessed.²⁴ This study found that ASCs and ASC-conditioned media both improved these metrics, with a moderate advantage using ASCs. Furthermore, ASC-derived vascular cells accounted for 9% of enhanced angiogenesis, suggesting that paracrine effects were largely responsible for the therapeutic function of ASCs versus repopulation.²⁴ The paracrine effects of ASCs have been suggested to modulate the microvasculature through cytokine secretions such as VEGF, IGF-1, bFGF, and SDF-1, as well as autocrine action and activation of resident stem cell populations.²⁵

An additional means by which ASCs exert their effects on microvasculature is by adopting a pericyte-like phenotype. When injected into rat mesenteries and assessed two months later by immunohistochemistry, 29% of hASCs showed perivascular morphologies. In addition, a portion of these hASCs also expressed pericyte surface markers NG2 and alpha-SMA.⁷ In a coculture model between ASCs and endothelial cells, endothelial cells were found to repress adipogenesis in ASCs through Wnt signaling and therefore stabilize vasculature.²³ An analysis of CD34+ adipose stromal cells revealed that more than 90% of these cells expressed mesenchymal, pericyte, and smooth muscle surface markers.²⁶ It is also possible that the mechanism of ASC

action is a combination of all of the above—differentiation, paracrine, and juxtacrine effects.

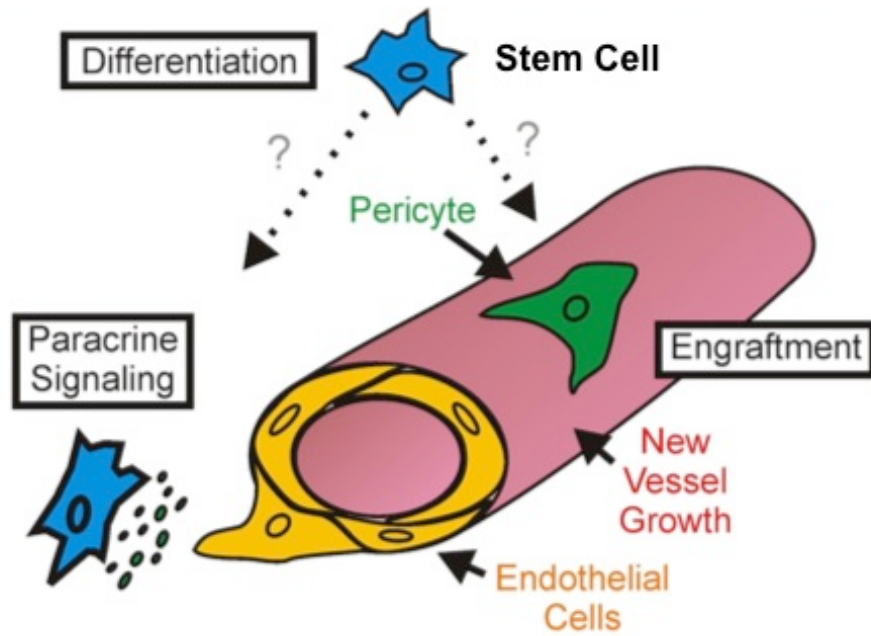


Figure 2: Putative mechanisms of ASC regeneration in vivo. ASCs are thought to act on endothelial cells and modulate vessel growth through a variety of putative mechanisms, including paracrine effects, differentiation, and engraftment.
Credit: Molly Kelly-Goss

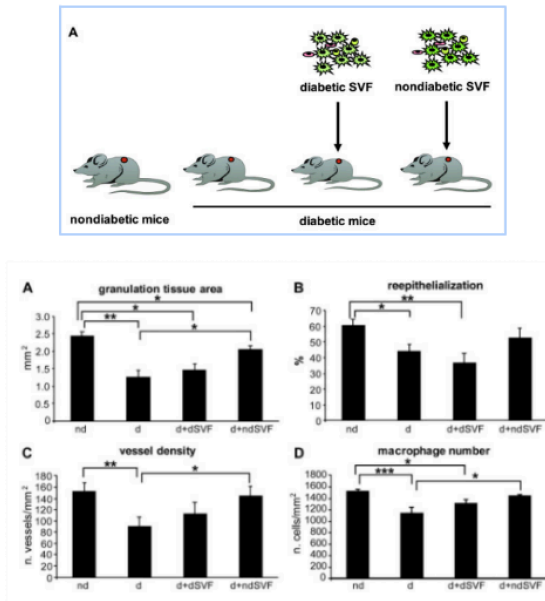
Autologous vs. Allogeneic ASC Transplant

ASCs are desirable because of their relative ease of harvest from accessible fat depots, as well as their potential for both allogeneic or autologous treatment.⁶ The use of autologously-derived ASCs has several advantages over allogeneic transplantation, including a reduced risk for infection, regulatory and histological compatibility, and the potential for immediate bedside or on-site processing.² Although allogeneically-transplanted ASCs have actually been shown to be immunosuppressive, these effects are not well documented.^{3,27} Since ASCs represent an important source of stem cells for therapy of diabetic complications, it is important to know the relative efficacies of autologous and allogeneic therapies for diabetic patients. However, only a few studies have examined whether ASCs obtained from diabetic patients are functionally impacted by the disease, pertaining to their role regenerative medicine (Figure 3).²⁸ To date, no studies have assessed the functional impact of diabetes on ASCs for the treatment of diabetic retinopathy.

Using a diabetic wound-healing model, Cianfarani et al. showed impaired ASC therapeutic potential in promoting wound healing when isolated from diabetic sources. In short, mice were rendered diabetic by STZ injection, and ASCs were isolated from these diabetic mice or non-diabetic mice.²⁹ The wound-healing model consisted of a biopsy punch through the skin of diabetic mice (also STZ-induced), onto which one of the two cell populations were administered. This group also performed a number of functional analyses, demonstrating decreased proliferation and migration in diabetic ASCs using BrdU incorporation and scratch assays, respectively, as well as decreased growth factor secretion using an ELISA. Finally, diabetic ASCs were shown to be impaired in facilitating keratinocyte proliferation.²⁹ Kim et al. reported similar findings using a rat hindlimb ischemia model in diabetic (STZ) rats.³⁰ The femoral artery was

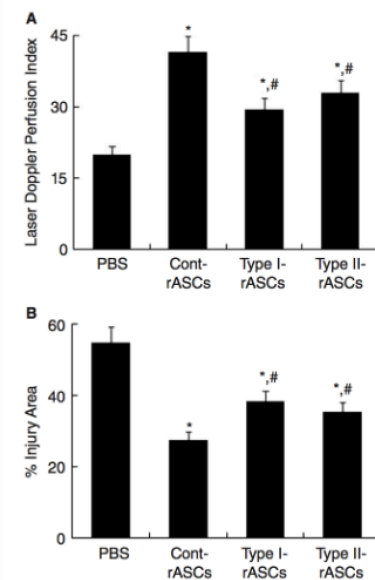
ligated to produce hindlimb ischemia, and ASCs obtained from diabetic rats, from non-diabetic rats cultured in high-glucose media, or from non-diabetic rats cultured in regular media were transplanted by injection. Blood flow was assessed two weeks later by laser doppler perfusion imaging. They showed that rASCs from diabetic sources resulted in a lower blood flow recovery compared to those from non-diabetic sources. rASCs cultured in high-glucose media showed a similar impairment.³⁰ A few other groups have performed functional analyses of ASCs derived from diabetic sources and in high-glucose environments. Samyra et al. showed that VEGF expression, proliferation, and tubulization ability was higher in ASCs from young, non-diabetic mice than aged non-diabetic mice, db/db mice, and mice injected with STZ.³¹ Cramer et al. compared the effects of high glucose on ASCs isolated from diabetic and non-diabetic human adipose tissue.³² They found that glucose lowers proliferation capacity and raises apoptosis frequency in diabetic ASCs more than in non-diabetic ASCs. Furthermore, glucose was shown to lower differentiation in the osteogenic and chondrogenic lineages, but facilitate differentiation towards adipogenesis.³²

Diabetic Wound Healing Model



Cianfarani et al. 2013

Hindlimb Ischemia Model (in non-diabetic rats)



Kim et al. 2008

Figure 3: Findings on Healthy vs. Diabetic ASCs from Other Studies. Cianfarani et al. (left) compared the ability of SVF from diabetic and non-diabetic mice to promote wound healing in diabetic mice, and found that SVF from diabetic mice were impaired in promoting wound closure. Kim et al. (right) performed a similar comparison using a non-diabetic animal model of hindlimb ischemia, and also showed impairment when using ASCs from diabetic animals.

Together, these results support the notion that ASCs from diabetic sources are functionally and therapeutically impaired, and it is important to investigate whether this impairment is also seen in the treatment of diabetic retinopathy. In addition, diabetic retinopathy presents a very different environment for ASCs from the wound healing and ischemia models that have been studied thus far. Using this disease model, we also expect to learn valuable information not only on the relative treatment efficacies of diabetic and healthy ASCs, but also on their differential behavior in vivo.

Diabetic Retinopathy

Diabetes profoundly impacts the microvasculature in nearly every tissue. Diabetic retinopathy is a striking example of this, and results in retinal capillary dropout, vessel leakage, and pathological neovascularization, leading to severe and irreversible vision loss. Figure 4 shows some of the most common clinical hallmarks of diabetic retinopathy. Current surgical and pharmacologic treatments are only effective at managing complications of diabetic retinopathy, but do not repair existing retinal damage.³³ Laser photocoagulation is the current treatment standard for proliferative diabetic retinopathy, and operates on the principle of cauterizing hypoxic retinal tissue.³⁴ While effective at stemming the progression of retinopathy, this procedure damages peripheral and night vision, often requires repeated treatments, and only prevents visual deterioration in half of cases.^{33–35} The destructive effects of laser photocoagulation can be seen in Figure 5, where scars cover much of the peripheral retina. Anti-VEGF therapy has been increasingly used alone or in combination with laser therapy, with improvements in vision loss due to diabetic macular edema.³⁶ However, anti-VEGF therapy requires frequent and painful intra-vitreous injections for several years, and unfortunately does not reverse the underlying pathology.³³ A lasting and non-destructive treatment for diabetic retinopathy is clearly needed.

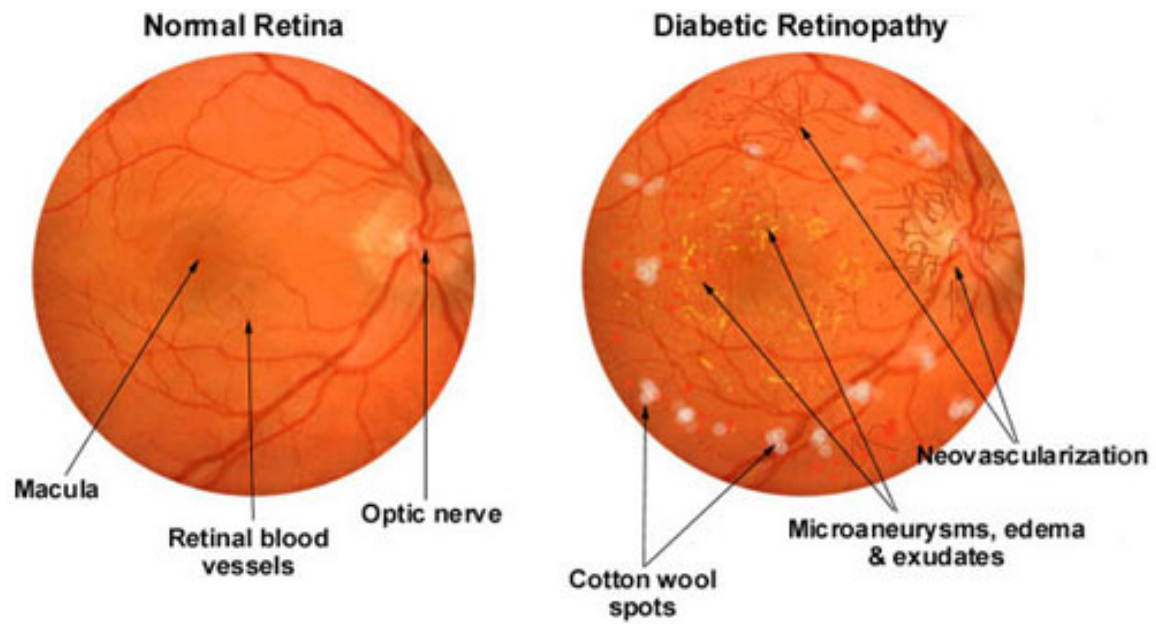


Figure 4: Clinical Hallmarks of Diabetic Retinopathy.
Source: www.eyerisvision.com

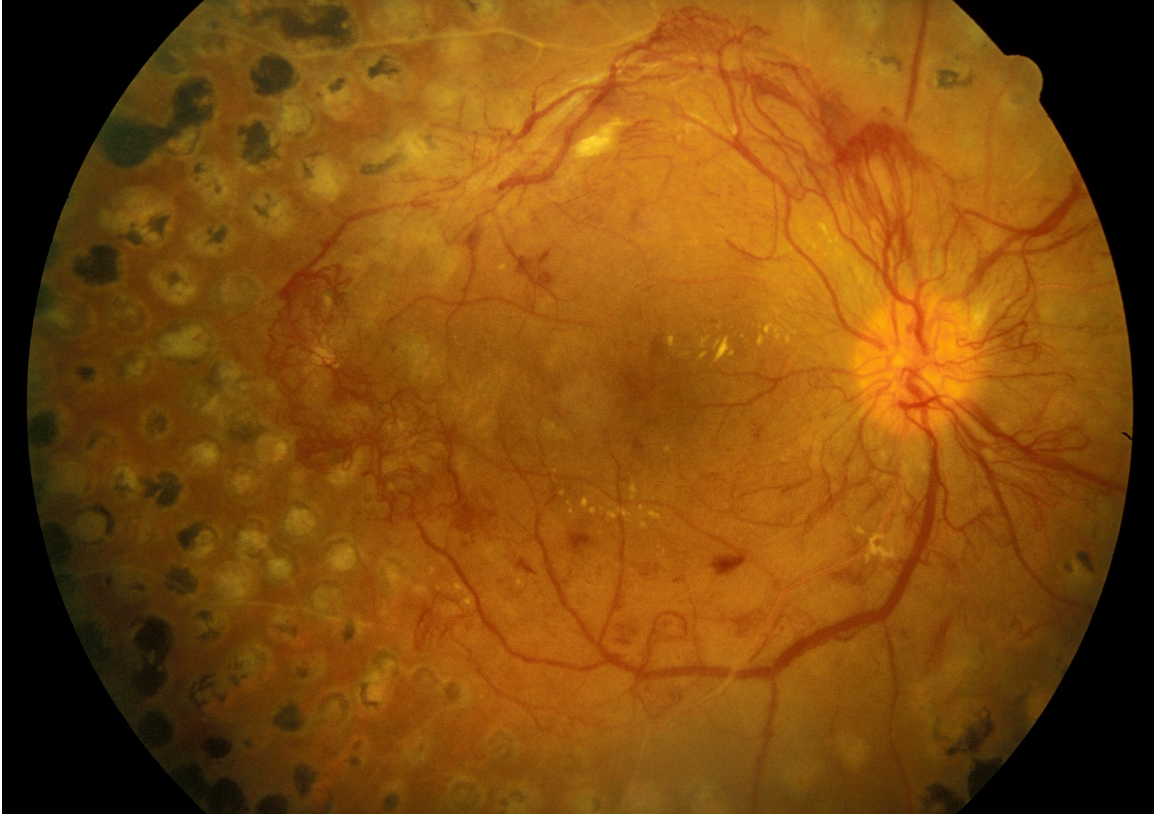


Figure 5: Peripheral Retinal Scarring from Laser Photocoagulation. Scar tissue can be seen on the left of the image, opposite the optic nerve, as light and dark circular lesions. Source: diabetesmanager.pbworks.com

Using the Akimba mouse model of diabetic retinopathy, we have probed the differences in treatment efficacy and function of mASCs derived from healthy vs. diabetic mice. The Akimba is a cross between the hyperglycemic Akita mouse, which carries a dominant negative mutation in its insulin 2 gene, and the Kimba mouse, which overexpresses human VEGF in retinal photoreceptor cells.^{37,38} The combination of these modifications creates a mouse whose retina exhibits hallmarks of proliferative diabetic retinopathy in humans with capillary dropout, retinal edema, and aberrant neovascularization.³⁸ In this study, we demonstrate that mASCs from healthy, non-diabetic mice are more effective than diabetic mASCs from Akimba mice in preventing vascular damage in the diabetic retina. To provide a mechanism for this observed difference in vasoprotective ability, a functional analysis of healthy and diabetic mASC was carried out. Several pro-angiogenic factors, including some known to effect retinal angiogenesis³⁹⁻⁴² were secreted at significantly higher levels in healthy versus diabetic mASCs. Furthermore, diabetic mASCs exhibited lower rates of proliferation and greater rates of apoptosis than healthy mASCs. These results indicate that diabetic ASCs are functionally impaired in treating murine models of diabetic retinopathy, and do not support the use of autologous ASCs from diabetic patients.

Methods

mASC Harvest and Culture

Isolation of the stromal vascular fraction from the epididymal fat pad and culture of mASCs was performed as detailed in Zuk et al 2001. Briefly, fat pads were harvested from 9-week old Akimba mice and non-diabetic (Akita^{-/-}) littermates, then digested in collagenase-containing (Sigma, St. Louis, MO) digestion buffer for one hour at 37C. The resulting mixture was filtered through 200-µm mesh to exclude any undigested tissue. The filtrate was centrifuged to remove remaining collagenase, and the pellet incubated with red blood cell lysis buffer (Sigma, St. Louis, MO) for 5 minutes at room temperature. The cell suspension was then sterile-filtered through 40-µm mesh and plated on sterile culture plates (Corning, Corning, NY). This process is shown in brief in Figure 6. Cells harvested from Akimba mice and non-diabetic littermates are referred to as “diabetic” and “healthy” mASCs, respectively.

mASCs were maintained in a sterile culture hood and incubator at 37 degrees C and 5% CO₂. Growth media consisted of 10% fetal bovine serum (Hyclone, Logan, UT) and 1% penicillin/streptomycin (Fisher Scientific, Waltham MA) in Dulbecco's Modified Eagle Medium (DMEM-F12) with added glutamate and sodium bicarbonate (Life Technologies). Cells were passaged at roughly 80% confluence, and media was changed every other day.

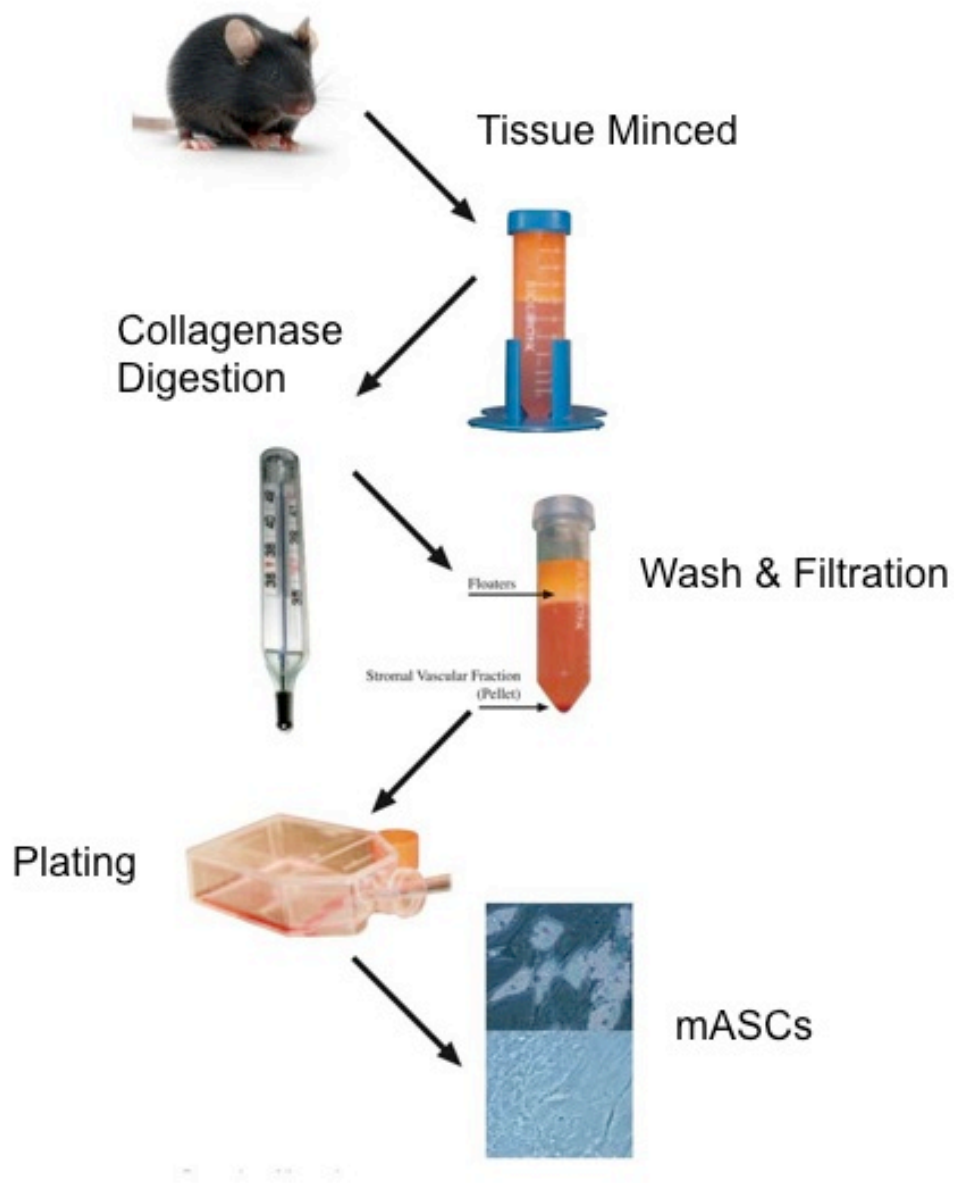


Figure 6: mASC harvest process. Adapted from Gimble et al. 2007.

Labeling and Intraocular Injection of mASCs

All animal studies were approved by the University of Virginia's Animal Care and Use Committee. Healthy mice were of the C57BL/6 strain, and diabetic mice were Akimba on the C57BL/6 background. Presence of the Akita genotype was detected by RT-PCR^{38,43} and hyperglycemia was confirmed by taking blood glucose measurements at 5 weeks of age using a OneTouch UltraMini blood glucose meter (LifeScan, Milpitas CA). Healthy and diabetic mASCs at passage 4 were fluorescently labeled with Vybrant DiI Cell-Labeling Solution (Life Technologies, Grand Island, NY) as per manufacturer's instructions, and resuspended in PBS at the appropriate concentration determined by hemocytometer. Each cell injection consisted of 10,000 mASCs suspended in 1.5 μ L of PBS. Control vehicle injections consisted of 1.5 μ L of PBS. Cells were resuspended by pipette immediately before injection of each eye to minimize cell clumping. Male 4 week old Akimba mice were anesthetized with ketamine/xylazine injected intraperitoneally and proparacaine (Fisher Scientific) applied topically to the eyes just prior to injection. mASCs were injected through the pars plana into the vitreous using a 33-gauge Hamilton syringe. A total of 12 Akimba mice were injected in this manner with mASCs in one eye and a contralateral PBS control injection in the other eye. In six of these mice, healthy mASCs were used, and in the other six diabetic mASCs were used. Figure 7 shows a timeline of this study, and Figure 8 shows a detailed layout of the experimental design.

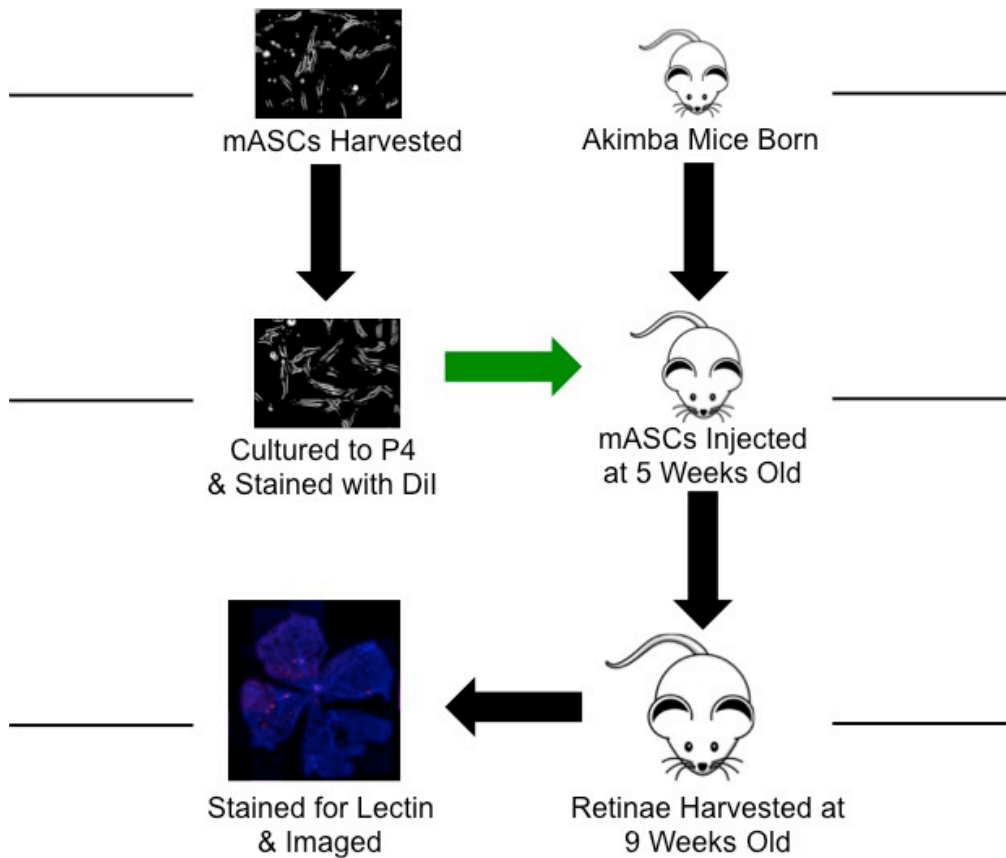


Figure 7: Timeline of in-vitro Akimba study. The study begins with the top line, where mice are born and cells are harvested (from different mice). Time progresses moving down the figure. Mouse image source: [vector.me](https://www.vector.me)

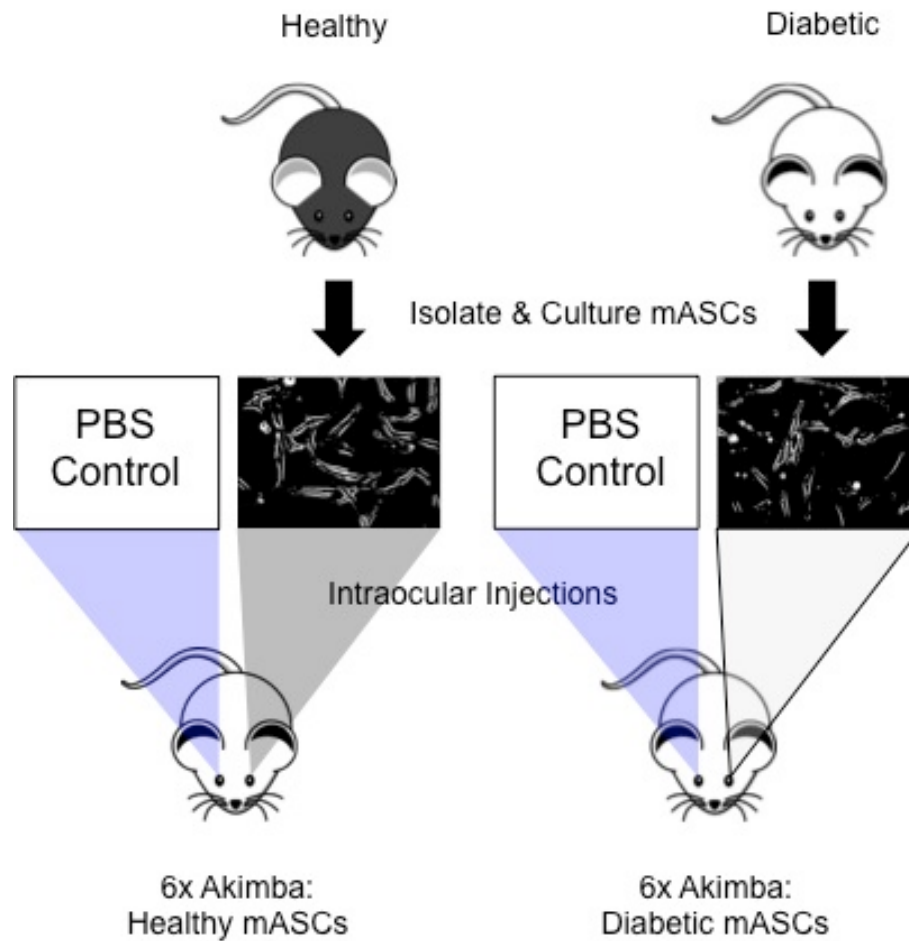


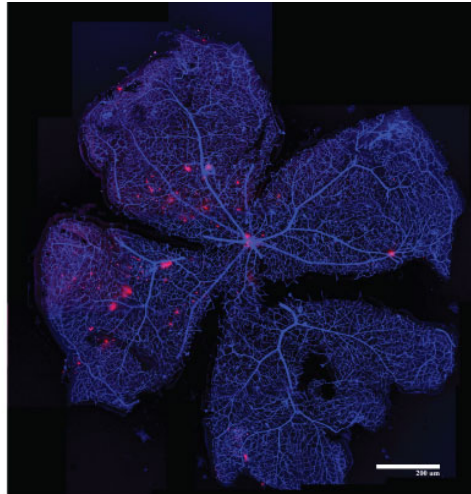
Figure 8: Detailed layout of Akimba study intraocular injections. mASCs were isolated from healthy and diabetic mice, and cultured separately. To additional groups of Akimba mice then received intraocular injections with one cell type (either healthy or diabetic) in one eye and a PBS contralateral control injection.

Retinal Whole-mounting and Immunostaining

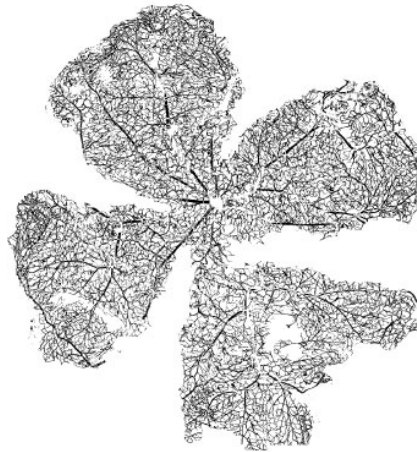
Treated mice were left for four weeks post-injection before harvesting retinæ. Mice were euthanized with carbon dioxide, followed immediately by cardiac perfusion-fixation by cutting the right atrium and injecting the left ventricle with 10 mL of 4% paraformaldehyde (PFA). Intact eyes were then removed and fixed by submersion in 4% PFA for 10 minutes. After rinsing the eyes with PBS, retinæ were isolated and whole-mounted on gel-coated slides. Retinæ were then permeabilized with 1 mg/mL digitonin (MP Biomedical, Solon, OH) for 1 hour and stained with mouse monoclonal AlexaFluor-647 (Life Technologies) overnight.

Imaging & Image Analysis: 10x, 20x, and 60x image stacks were taken on a Nikon (model #) confocal laser scanning microscope. 10x stacks were flattened and tiled into whole-retina montages using ImageJ. Vessel length of whole retinæ was calculated digitally by skeletonization in ImageJ and subsequent pixel count of the skeletonized vasculature in MATLAB (version 2013a). Briefly, ImageJ converted vascular network images to binary skeletonized images. Each black pixel was counted as vessel, and each white pixel was counted as non-vessel area in MATLAB. Vascular density is equal to the ratio of vessel length to whole retina area. This process is summarized graphically in Figure 9. Labeled mASCs were counted in three representative 20x image stacks per retina by blinded observers. Each field of view was taken at the same distance from the optic nerve. An example of such a 20x image and cell counting is shown in Figure 10.

Original Immunofluorescent
Image



Binary Image



Skeletonized Vessel
Network

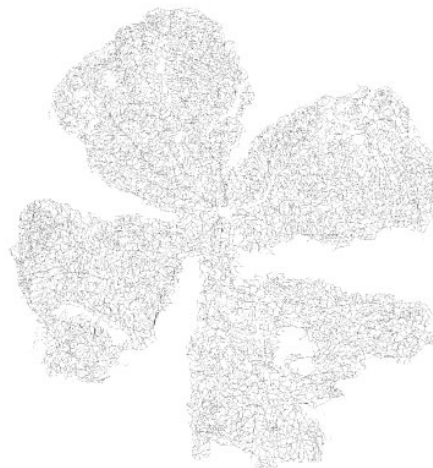


Figure 9: Image processing procedure. (Top) Image of a whole-mounted immunostained retina created by stitching 10x tiles together. (Middle) Fluorescent image binned into vessel (black) and non-vessel area (white). (Bottom) Binned image skeletonized to produce a the image shown with all vessels represented by one pixel-width line.

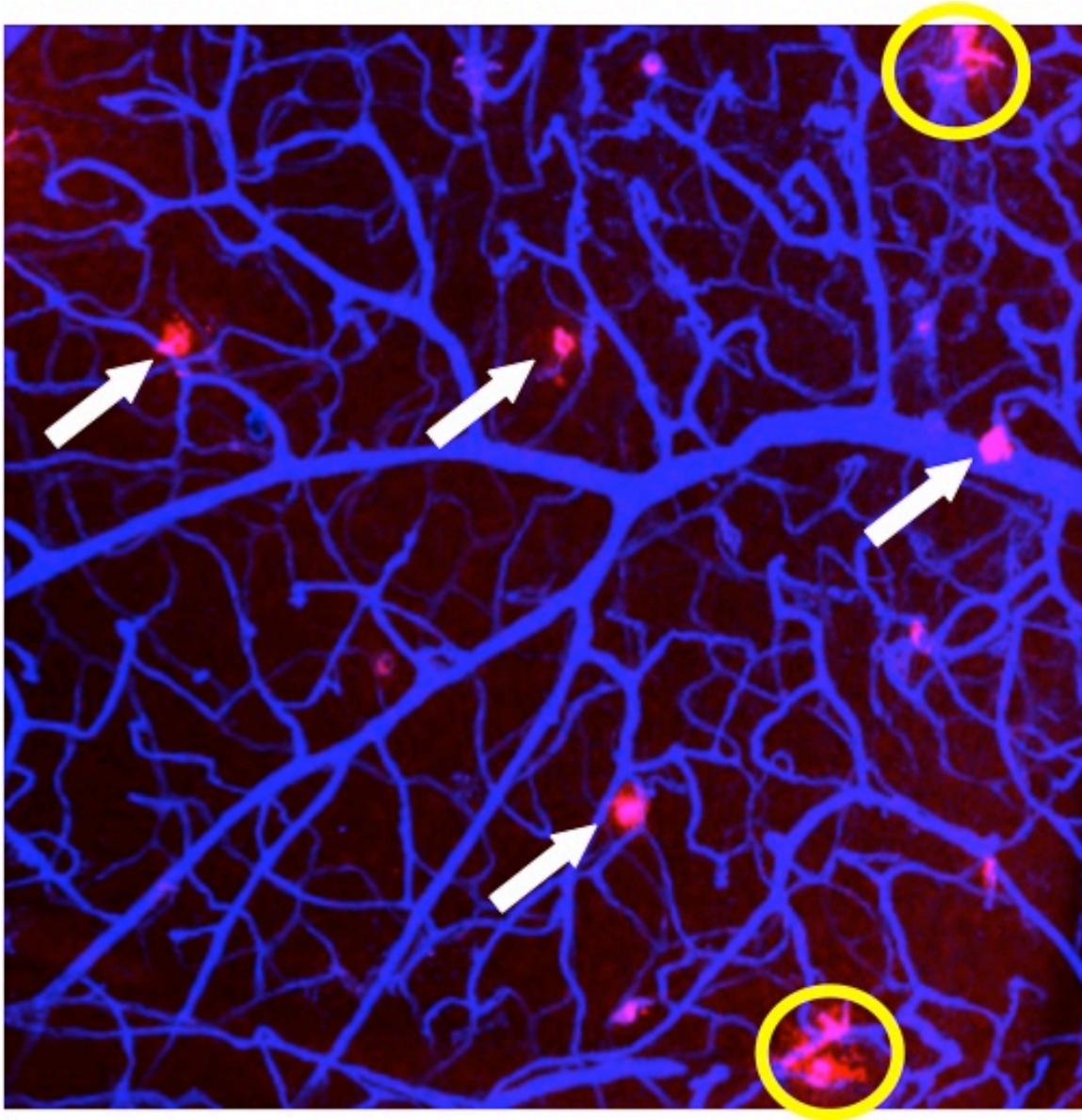


Figure 10: Method of counting labeled mASCs. Sample 20x field of view shown above. White arrows indicate examples of cells, yellow circles indicate examples of excess/diffuse Dil that would not be counted as cells by the blinded observer.

Monte Carlo Simulation: A Monte Carlo simulation was created in MATLAB to determine the random placement of mASCs on retinal vasculature. The simulation used binary images of fluorescent retinal vasculature micrographs (20X magnification) to generate a matrix of coordinates for the retinal vasculature. For each micrograph, a random matrix of mASC coordinates was generated. Identical retinal vasculature coordinates and mASC coordinates were counted to determine the probability of mASCs randomly contacting retinal vasculature after random distribution. See Figure 11 for a demonstration of this process. The simulation was looped 1000 times for more accurate probability calculations. Utilizing Delaunay triangulation, the simulation also created a histogram to visualize the probability distribution of the distance of randomly simulated mASCs from retinal vasculature.

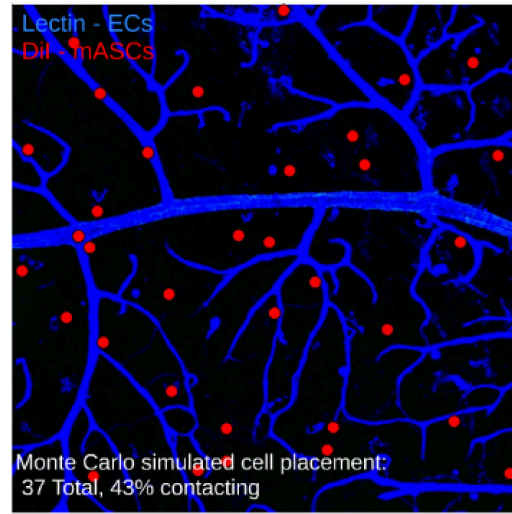
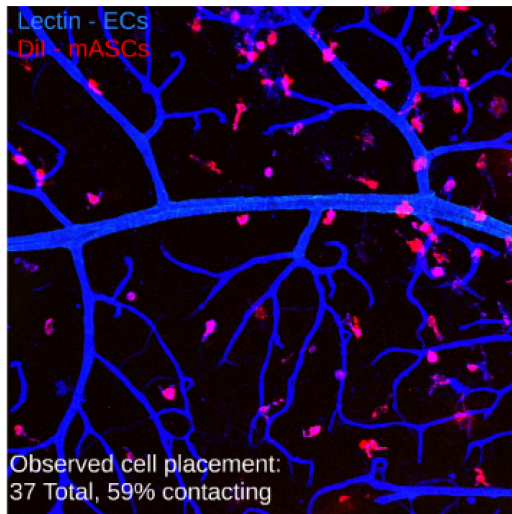


Figure 11: Sample Monte-Carlo simulation processed image. Original fluorescent 20x image shown to the left with 37 total cells counted by the blinded observer and 59% of these cells in contact with vessels. Processed image shown on right, with an equal total number of cells in the field of view, but only 43% of simulated cells falling in contact with vessels.

Angiogenesis Secretome: Conditioned media samples were obtained from 3 populations each of healthy and diabetic mASCs, taken from wild-type and Akimba mice of the same age, respectively. All cells were simultaneously passaged to P4, counted, plated with fresh media, and allowed to incubate at 37°C for 24 hours before collection of conditioned media. These samples were run on a Mouse Proteome Profiler Angiogenesis Array (RnD Systems ARY015), which tested for 53 angiogenic factors. X-ray film captured chemiluminescence from each dot, which was proportional to the amount of factor bound. Relative expression levels were obtained from densitometry analysis (ImageJ) of x-ray film spots. Finally, angiogenic factor levels were normalized to positive control and cell count.

Measurements of oxygen consumption and mitochondrial function: Oxygen consumption rate (OCR) was measured using a Seahorse XF-24 Flux Analyzer (Seahorse Biosciences, Billerica, MA), as previously described ¹. mASCs were seeded in a Seahorse 24-well tissue culture plate at a density of 3.0×10^4 cells/well in normal growth media for 24 hours prior to the assay. On the day of the assay the media was changed to unbuffered DMEM and equilibrated at 37°C. Oligomycin (2 μ M), FCCP (1 μ M), and Rotenone and Antimycin A (1 μ M and 10 μ M) were injected sequentially during the assay as indicated. Each OCR measurement represents the average of a 3 minute reading every 10 min, with 3 min of mixing and 4 min of wait time per cycle. 3-4 wells were used for each experimental group.

Cell Force Measurements

Measurements of total cell contractile force were carried out as described in (Yang, Fu et al. 2011). Briefly, mASCs were plated at a density of 5000 cells/cm² on micropost

substrate arrays. After allowing to adhere for 7 minutes, non-adherent were washed off and plates were inspected to ensure a majority of cells were occupying isolated positions without cell-cell contacts. Cell culture media was replaced and cells allowed to continue adhering overnight. Cells were fixed using a 4% paraformaldehyde solution for 20 minutes and then stained with Alexa Fluor 488 Phalloidin (Molecular Probes) to observe the f-actin cytoskeleton. Confocal images of micropost “top” positions and cell outlines were analyzed in MATLAB to generate force maps and calculate total cell force on a cell-by-cell basis.

Cell Proliferation & Apoptosis Assays

mASCs from three 9 week old healthy and three 9 week old diabetic Akimba animals were plated on glass coverslips in 12-well dishes at a density of 4000 cells/cm² and allowed to adhere for 24 hours (Cold Spring Harbor proceedings). Three coverslips were cultured for each animal. To measure cell proliferation in each population of mASCs, mASCs were incubated with 5-ethynyl-2'-deoxyuridine (EdU) for 12 hours and subsequently stained following the manufacturer's instructions. To measure apoptosis, the terminal deoxynucleotidyl transferase dUTP nick end labeling (TUNEL) method was used. Fluorescence intensity from both EdU and TUNEL assays was measured for each coverslip using confocal microscopy, taking image stacks with a 3µm spacing and measuring total fluorescence intensity for each coverslip in ImageJ.

Statistical Analysis

In vivo studies were analyzed for numerical differences using paired t-tests comparing left and right eyes for 6 healthy and 6 diabetic animals. All *in vitro* mASC experiments were performed with 3 healthy and 3 diabetic animals, and significance was determined using a student's t-test. Statistical tests including t-tests, paired t-tests, Wilcoxon Signed

Rank tests, and ANOVAs were performed in SigmaStat (Systat Software Inc, San Jose, CA). Statistical significance was determined using a maximum p-value of 0.05 or smaller if indicated.

Results

Regenerative Potential

Using the Akimba murine model of diabetic retinopathy, we tested whether hyperglycemia alters mASCs ability to protect the diseased microvasculature in the Akimba retina. The Akimba retina demonstrates several hallmarks of proliferative diabetic retinopathy in humans, including retinal thinning and severe vascular pathology such as capillary dropout, nonperfusion, retinal neovascularization, retinal edema, and microaneurysms.³⁸ mASCs used for treatment were harvested from either 9 week old hyperglycemic Akimba mice or non-diabetic littermates both on a C57BL/6 background. Each mouse received injected mASCs in one eye (either healthy or diabetic) and a contralateral PBS vehicle control. Four weeks later, retinæ were harvested and immunostained. Confocal images of isolectin-stained retinæ and Dil-labeled injected mASCs are shown in Figure 12A and C. The greater loss of capillaries in diabetic mASC-treated retinæ compared to healthy mASC-treated retinæ is visually apparent. To quantify this difference in treatment outcome, vascular density was calculated digitally by the ratio of total vessel length to total retinal area. The change in vascular density of mASC-injected eyes minus that of control eyes is shown graphically in Figure 1. To correct for variability in disease severity between individual mice, all analysis on vascular density was performed by comparing the mASC-treated retina to the control PBS-injected retina in the same mouse. A majority of eyes treated with diabetic mASCs had a lower vascular density compared to contralateral controls (Figure 12A and B). When considering the overall change of vascular density, diabetic mASC-treated eyes

displayed both increases and decreases in vascular density with no meaningful trend. Meanwhile, those treated with healthy mASCs showed a significant increase in vascular density relative to contralateral controls (Figure 12C & D). These data indicate that diabetic mASCs are not as effective as healthy mASCs in promoting protection against vascular dropout in the Akimba retina.

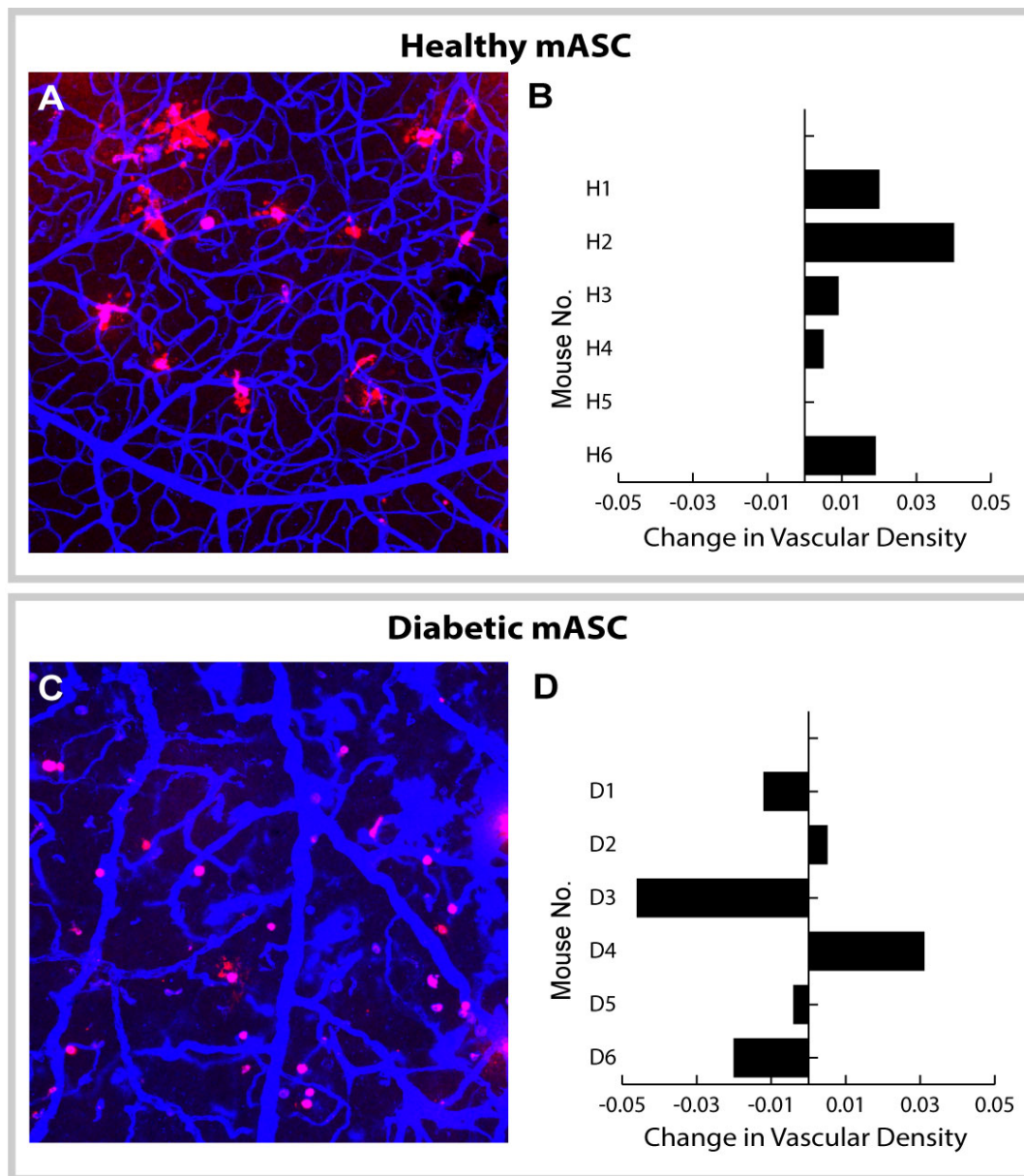


Figure 12. Treatment with healthy and diabetic mASCs have differential effects on the retinal microvasculature. 5-week old Akimba mice received intraocular injections of “healthy” or “diabetic” passage-4, Dil-labeled mASCs in the right eye and contralateral phosphate-buffered saline control injections in the left eye. 10x confocal microscopy images with mASCs in red and lectin-stained vessels in blue of healthy cell-treated (A) and diabetic cell-treated (C) retinæ. Differences in vascular densities for each mouse between cell-treated retinæ and contralateral PBS controls showed no change in diabetic cell-treated (B), and a significant increase in healthy cell-treated (D), $n = 6$, $p < 0.05$, paired t-test.

Retinal Incorporation

As seen in Figure 12A and C, it was possible to observe Dil-labeled mASCs in retinas harvested four weeks after cell injection. The number of mASCs that incorporated into the retina per field of view did not significantly differ between healthy and diabetic mASCs (6.77 healthy cells per field of view, 6.73 diabetic cells per field of view).

Perivascular Incorporation

To better understand how the injected mASCs were distributed spatially in the retina, and identify any preference of mASCs to incorporate in perivascular positions, each Dil-labeled cell was sorted as either perivascular or non-perivascular by a blinded observer. This was done for eyes treated with healthy and diabetic mASCs, and the results are shown in Figure 13. Healthy mASCs were found in perivascular positions more often than non-perivascular positions. Diabetic mASCs were found in relatively equal abundance both in perivascular and non-perivascular positions. To determine whether the injected mASCs preferentially resided in perivascular positions, or were localized there by chance, we carried out a Monte Carlo simulation on each 20x field of view. This stochastic simulation provided an estimate of the number of cells for each given field that one would expect to find in contact with a vessel by chance alone (Figure 14). The simulation generally predicted higher percentages of perivascular cells for healthy cells than diabetic cells, in accordance with observed results described in Figure 13. However, a higher number of points are found on the upper left side of the diagonal for both healthy and diabetic cells, indicating that the number of mASCs found within perivascular distance was greater than what we would expect due to chance alone for both cell populations.

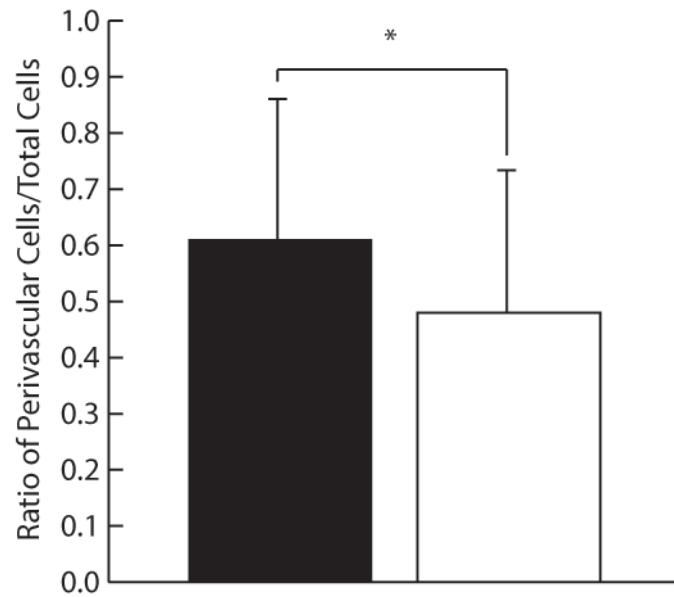


Figure 13: Healthy mASCs incorporate in the retina in greater numbers and assume perivascular positions more often than diabetic mASCs. Cells occupying perivascular and non-perivascular positions counted in representative 20x confocal image stacks. The average ratio of perivascular cells to total cells in each field is shown for both healthy and diabetic cells. $n = 16$ (healthy), $n = 19$ (diabetic), $*p < 0.05$, Wilcoxon Signed Rank test.

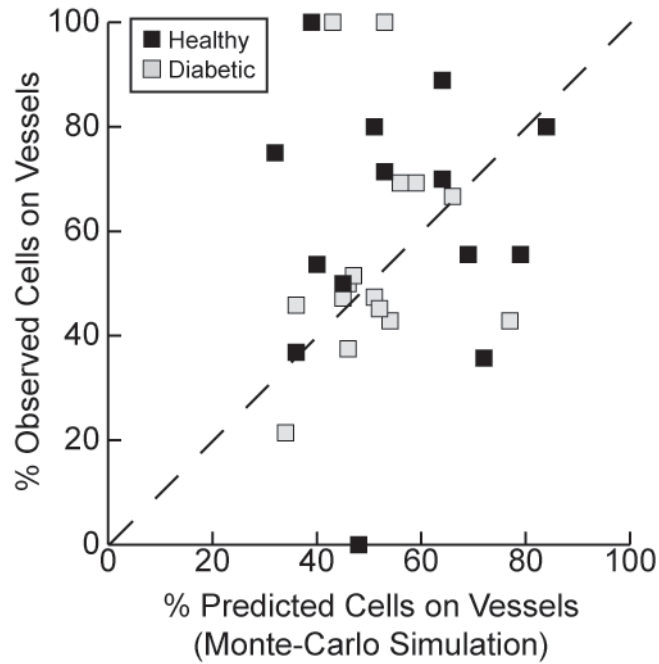


Figure 14: Stochastic analysis of mASC spatial distribution in the retina reveals a preference of mASCs to incorporate near vessels. Each analyzed 20x confocal image is represented as a dot, with the model-predicted percentage of perivascular cells for each image on the x-axis, and the percentage actually observed on the y-axis. At the dashed line ($y = x$), the observed percentage of perivascular cells is exactly what would be expected due to chance. Above this line, a greater number of perivascular cells were observed than expected by chance, and below the line, fewer were observed than expected by chance.

mASC Viability and Apoptosis Analysis

Relative rates of proliferation and apoptosis between healthy and diabetic mASCs were quantified in-vitro with cultured mASCs. Proliferation frequencies were measured using an EdU-incorporation assay (Life Technologies etc). We found that diabetic mASC proliferation activity was $77 \pm 5\%$ that of healthy mASCs (Figure 15A). Diabetic mASC apoptosis activity was $121 \pm 3\%$ that of healthy mASCs as determined by a TUNEL assay (Figure 15B).

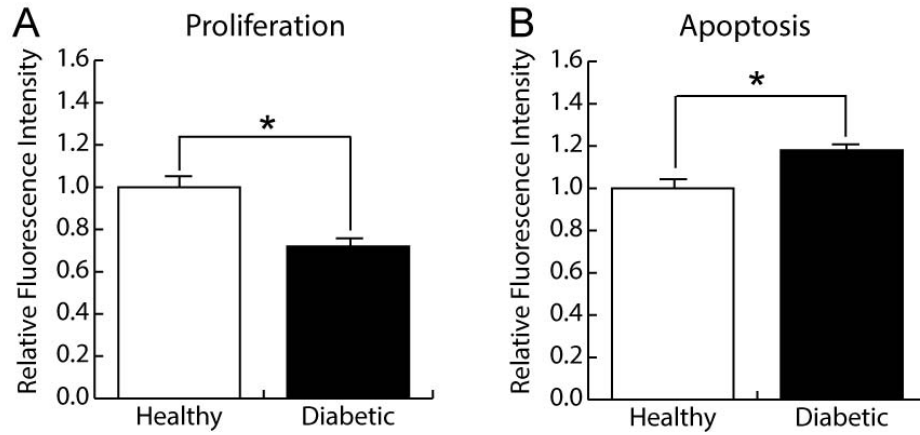


Figure 15: Healthy mASCs exhibit higher rates of proliferation and lower rates of apoptosis than diabetic mASCs. A. Relative number of cells in S phase determined by EdU incorporation assay. B. Cells undergoing apoptosis determined by TUNEL assay. mASCs from 3 healthy and 3 diabetic animals were used for each condition, with three cell plates per animal. Values were normalized to the healthy value in each case. * $p < 0.001$, t-test.

mASC Cellular Bioenergetics & Cell Force Measurements

An analysis of the two mASC populations' bioenergetic profiles was then performed using the Seahorse instrument to determine whether differences in cellular metabolism may account for their differing treatment efficacy and function *in vivo*. Specifically, we assayed mitochondrial bioenergetics in whole cells by measuring oxygen consumption over time following the sequential addition of the ATP synthase inhibitor oligomycin, the mitochondrial uncoupler FCCP, and the complexes I and III inhibitors rotenone and Antimycin A¹. These data revealed that diabetic and non-diabetic mASCs had comparable rates of basal cellular respiration, ATP-dependent respiration, spare respiratory capacity, uncoupled respiration, and non-mitochondrial respiration (Figure 16). Cell contractile force was also quantified using micropost arrays and subsequent analysis using confocal microscopy. This analysis revealed no significant differences in contractile force generation between healthy and diabetic mASCs (Figure 17).

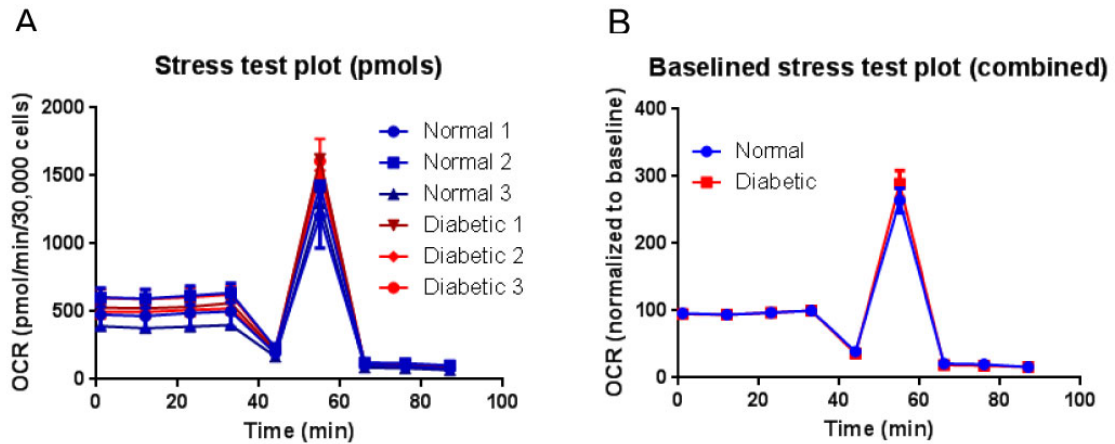


Figure 16: Healthy and diabetic mASCs show no difference in metabolic activity. Healthy and diabetic mASCs were isolated from three diabetic mice and three healthy mice, passaged to P4, and subjected to mitochondrial stress tests on the Seahorse XF Bioanalyzer. Individual profiles (A) and combined profiles (B) show no difference in baseline cellular respiration, spare respiratory capacity, ATP-linked respiration, uncoupled respiration, or non-mitochondrial respiration.

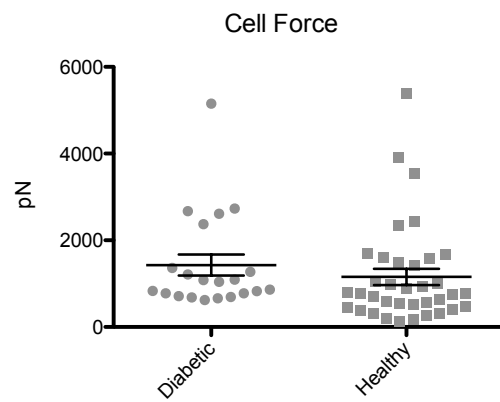


Figure 17: Total cell force of diabetic and healthy mASCs is not significantly different. Data displayed are Mean \pm SE, N = 21 Diabetic Cells, N = 36 Healthy Cells.

Angiogenesis Factor Secretome

To investigate a possible paracrine signaling basis for the differences in the potential of healthy and diabetic mASCs to protect against vascular dropout, levels of secreted angiogenic factors were measured via high-throughput ELISA. Conditioned media samples were collected from three populations each of healthy and diabetic mASCs. Each sample was run on a separate array under identical conditions, which enabled us to calculate a relative abundance of each angiogenesis factor by comparing arrays after normalizing to a positive control. Since healthy mASCs were found to proliferate faster than diabetic mASCs in culture, angiogenesis factor levels were also normalized to cell number as counted immediately prior to collection of conditioned media. We found 5 angiogenic factors that were secreted at significantly higher levels by healthy mASCs than by diabetic mASCs, namely IGFBP-2, IGFBP-3, MCP-1, osteopontin, and SDF-1 (Figure 18). The remaining factors of the 11 analyzed were secreted at similar levels by healthy and diabetic mASCs, and none were secreted at higher levels by diabetic mASCs.

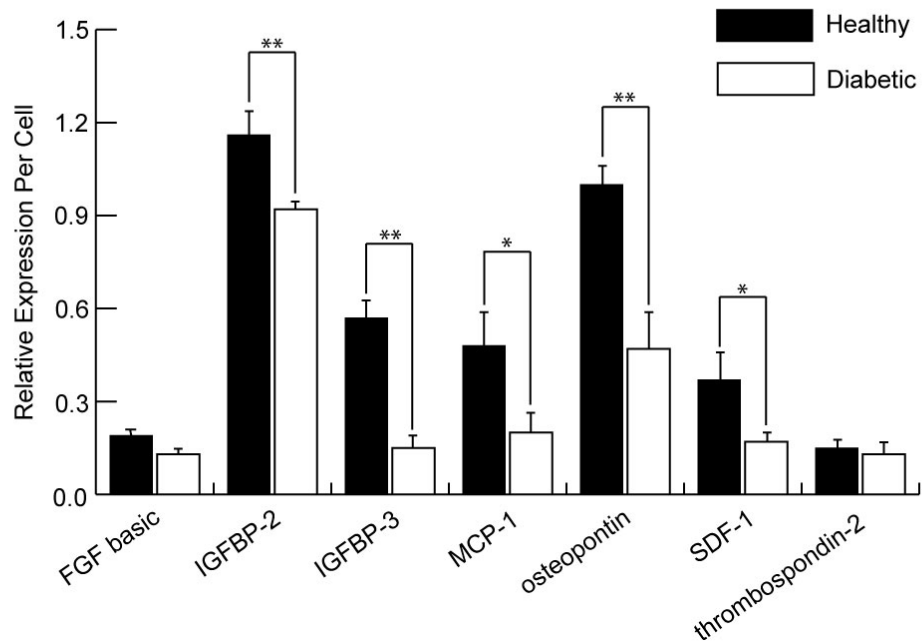


Figure 18. Diabetic mASCs secrete lower levels of angiogenic factors. Relative expression levels of secreted angiogenesis factor of healthy versus diabetic mASCs were taken using high-throughput ELISA arrays. mASCs were isolated from “healthy” wild-type and “diabetic” Akimba mice and maintained to passage 4. Samples consisted of conditioned media obtained by incubating cells immediately after passage in fresh media, and collecting media after 24 hours. $n = 3$, $*p < 0.05$, $**p < 0.01$, t-test

Discussion

ASC therapy holds promise for many debilitating and increasingly common vascular disorders due to their stabilizing effects on the microvasculature. This has been attributed to the ability of ASCs and other stem cell types to release angiogenic cytokines and to differentiate into vascular and vascular support cells.^{44,45} Furthermore, isolation of ASCs has several advantages over other cell types due to the relative abundance of adipose tissue and relatively painless extraction procedure.⁴⁶ The fact that ASCs can be rapidly isolated at high enough quantities for treatment without culture and expansion holds great implications for autologous treatment options. Thus, it is important to assess whether or to what extent ASCs isolated from a diabetic source have compromised treatment efficacy and function.

In this study, we first demonstrated that mASCs from diabetic sources are not as effective as those from healthy sources in protecting against vascular dropout in diabetic retinopathy (Figure 19). In addition to highlighting the effect of diabetes on mASCs treatment efficacy in vivo, this experiment corroborated our group's previous findings that healthy ASCs regenerate damaged retinal microvasculature. In contrast to the current study, these previous results were obtained using the oxygen-induced retinopathy model in immunosuppressed mice, and with ASCs isolated from only non-diabetic human adipose tissue.²² In an effort to explain the observed decreased treatment efficacy when using ASCs from diabetic sources, we carried out an analysis of mASC incorporation in vivo, and an in vitro functional analysis. We found that mASCs from diabetic sources undergo proliferation less frequently and apoptosis more frequently, in accordance with other functional studies using diabetic mASCs.² Analyses of mASC bioenergetics and force generation revealed no differences between healthy and diabetic mASCs. However, mASCs from diabetic sources secreted lower levels of angiogenesis-promoting factors.















Function	Healthy mASCs	Diabetic mASCs
Stabilize Retinal Vasculature		
Perivascular Incorporation		
Proliferation		
Angiogenic Factor Secretion		
Contractile Force		
Metabolism		
Apoptosis		

Figure 19: Summary of findings for Healthy vs. Diabetic mASCs. The direction of the arrows indicates the change in these functions relative to the other cell type. The color represents the putative impact on vascular stabilization.

The observed differences in mASCs isolated from healthy and diabetic sources have implications for the use and study of stem cells beyond the model disease in this study. Based on the fact that diabetic mASCs are impaired in their regenerative ability to the point that their use did not elicit a predictable and positive response in vivo, an autologous approach to ASC therapy in diabetic patients cannot be recommended without considering and possibly correcting for these differences. Furthermore, the greater levels of angiogenesis factor secretion in healthy mASCs and concomitant increase in microvascular regeneration supports the notion that ASCs act on surrounding tissues through paracrine activity. Several studies have found that the regenerative effects of mesenchymal stem cells (MSCs) are at least in part due to the release of paracrine factors,⁴⁷⁻⁴⁹ which act on the microvasculature by facilitating endothelial progenitor cell homing and restructuring vascular networks.⁵⁰ A comparison of diabetic and healthy embryonic stem cell function using a hindlimb ischemia model also determined that the loss of function and treatment efficacy was due to lower angiogenic factor secretion by diabetic ESCs.⁵¹

It is interesting to note that while diabetic mASCs showed decreased secretion of these angiogenic factors as well as functional impairment, the impairment was not universally seen in all aspects of cell function. Specifically, metabolic capacity, mitochondrial function, and contractile force generation were identical in healthy and diabetic cells, suggesting diabetes-associated hyperglycemia had no lasting effect on these functions. While others have reported significant hyperglycemia-induced changes in metabolism in other cell types such as bovine retinal pericytes, these studies were performed using high-glucose media.⁵² The fact that we saw no metabolic differences after culturing cells to P4 indicates that these differences were likely transient, in contrast to angiogenesis factor secretion, which was persistent. Recent evidence implicates

epigenetic modification as a driving force in diabetic microvascular complications, which are thought to lead to dysregulation of oxidant and pro-inflammatory factors, and promote vascular inflammation.^{53–55} MSCs are well known for their anti-inflammatory role,⁵⁶ and have been hypothesized to transition between multiple states in response to local cues during infection and wound healing.⁵⁷ The mechanism of epigenetic modifications in MSCs or ASCs in response to hyperglycemia is as of yet unknown, but it is possible that these modifications cause similar pro-inflammatory changes in ASCs, and are responsible for the observed differences in cell survival and cytokine secretion.

Pericytes belong to the vascular smooth muscle cell lineage, and are known to communicate with endothelial cells through direct cell-cell contact, and regulate blood flow through contraction and relaxation.⁵⁸ ASCs have been found to have many similarities with pericytes, such as expressing pericyte surface markers, taking up a perivascular location, and stabilizing endothelial networks.²⁶ An absence of pericytes, such as in the pathogenesis of diabetic retinopathy, leads to dysfunction of endothelial cell junctions and abnormal vessel morphology.⁵⁹ MSCs are thought to be closely connected with perivascular cells,^{50,60} and ASCs have been shown to originate from perivascular MSCs which reside in great numbers in adipose tissue.¹¹ This would suggest that ASCs might exert their vascular-stabilizing effects by taking up perivascular positions. Our results combining in vivo data with a stochastic model of mASC placement showed a slight preference of both healthy and diabetic mASCs to incorporate in perivascular locations, potentially by chemotaxis or other homing mechanisms. Analysis of our in-vivo data indicated a significantly higher number of healthy mASCs were in contact with vessels than diabetic mASCs. Taken together, these results suggest that the homing behavior of ASCs may be an intrinsic behavior that is diminished, but not abolished in diabetic cells. While interesting, our ability to draw conclusions about ASC homing is limited by the nature of our study. Further

investigation into the migration of mASCs in the retina in the form of live imaging would be invaluable in further characterizing any homing behavior of mASCs towards vessels.

In summary, we have shown that ASCs taken from diabetic sources impairs their ability to stabilize the microvasculature in diabetic retinopathy, and that use of autologously-derived ASCs from diabetic patients would not be effective. Furthermore, hyperglycemia causes distinct changes in ASC function, but only to certain aspects related to regulation of inflammation and angiogenesis. Finally, our results support the notion that ASCs promote vascular regeneration through paracrine activity rather than direct cell-cell contact.

Future Directions

Mechanism of Action

To improve ASC therapy for diabetic retinopathy and for stem cell therapy in general, it is critical to better understand both how endogenous stem cells are affected in the disease and the mechanism of transplanted ASC action in vivo. The current theory on the molecular basis of diabetic complications holds that endothelial cell, endothelial progenitor cell (EPC), and pericyte dysfunction all play key roles in the progression of these complications.²⁸ Endothelial cells are directly exposed to high serum glucose levels, and accumulate abnormally high glucose levels themselves. Unregulated glucose uptake leads to a variety of cellular changes, such as aberrant production of ECM proteins, over-activation of MAPK and related pathways, and overproduction of reactive oxygen species (ROS). These molecular events in turn result in endothelial cell apoptosis and loss of pericytes, and eventually to the formation of acellular capillaries and ischemia in the effected tissue.

While dysfunctional endothelial cells are thought to be the primary effectors of vascular pathology in diabetes, there is mounting evidence that local stem cell

populations have significant contributions as well. A reduction of 44% of circulating EPCs was observed in type 1 diabetic patients, as well as decreased angiogenic ability.⁶¹ In type 2 diabetic patients with peripheral arterial disease, a reduction of 53% was observed.⁶² Furthermore, EPCs from diabetic sources have reduced capacity to adhere to an endothelial cell monolayer in vitro.⁶³ Pericytes share an equally prominent role in the pathogenesis of diabetic complications. The loss of pericytes is correlated with several devastating disorders, such as fibrogenic kidney disease, Alzheimer's, and diabetic retinopathy. These findings strongly implicate native pericytes and EPCs in diabetic complications. It has long been appreciated that endothelial cell ROS overproduction is loosely to blame for their loss and dysfunction,³⁵ but the precise mechanisms are not at all well characterized.⁶⁴ Recent studies have suggested that the link between mural cell loss and hyperglycemia is more complex than initially anticipated, and that retinal pericytes themselves harbor morphologically distinct subpopulations that are each affected differently by the disease.⁶⁵

The hypothesis that all MSCs are pericytes has been gaining increased acceptance.⁶⁶ As previously discussed, several examples including the present study have demonstrated functional deficiencies in stem cell populations from diabetic sources. Integrating these two conclusions suggests that stem cells are damaged in diabetes in a similar if not indistinguishable manner to pericyte loss in diabetes. Trying to repopulate perivascular positions with cells that possess no more inherent resistance than their predecessors to local inflammation may be an uphill battle that would explain the promising, but ultimately modest success of stem cell therapies in microvascular complications. Being fully aware of the precise failure point(s) in the interactions of stem & progenitor cells, pericytes, and endothelial cells that arise in disease will be necessary to eventually develop a cell-based treatment that addresses them in any curative or lasting fashion.

Stem Cell Pre-Conditioning/Reprogramming

The environment of tissues in which ASCs and other stem cell therapies are aimed are often subject to elevated inflammation, ischemia, and other factors that present unique therapeutic targets.⁶⁷ Simply using a freshly-isolated, unmodified population of stem cells may not always be the most effective treatments for all of these targets. Pre-conditioning or re-programming stem cells with growth factors or cytokines represent accessible ways to customize stem cell populations and enhance their effects for a specific use. Pre-conditioning MSCs with paracrine factors such as TGF-beta or SDF-1alpha has been shown to improve cardioprotective effects in models of myocardial infarction by enhancing cell survival and angiogenesis.^{68,69} Our group has demonstrated the positive effects of TGF-beta pre-conditioning on ASCs in the treatment of oxygen-induced retinopathy.²² Pre-conditioning with SNAP ((S-nitroso N-acetyl penicillamine) enhanced their regenerative effects in renal ischemic injury by promoting survival, engraftment, proliferation, and decreasing fibrosis.⁷⁰ Other diverse methods of pre-conditioning also exist. Hypoxia preconditioning has been shown to increase production of pro-survival transcription and growth factors, and perform better when transplanted in myocardial infarction models.⁷¹ Exposure to nitric oxide and hyperthermia have both been shown to enhance survival and paracrine activity, and engraftment success, respectively.^{67,72,73}

Individualized care is a sought-after idea that complex, versatile, and self-contained stem cells may one day be well suited for. Pre-conditioning approaches will be invaluable in increasing the effectiveness and specificity of cell-based therapies moving forward. As we continue to improve our understanding of the intra-cellular pathways and cell-cell interactions most responsible for angiogenesis, cell survival, and other desired

functions, we will be able to better mold stem cell populations to have desired properties and capabilities as needed.

Connections to Dentistry

The potential of stem cell therapy has grown to encompass diverse applications and fields, for example in dentistry. Bone loss is a common problem in cranio-maxillofacial surgery and periodontics that can lead to the loss of the supported teeth if left untreated.⁷⁴ The current standard of treatment is bone grafting, a surgery which carries a high incidence of complications and the need for a second surgery.⁷⁵⁻⁷⁷ ASCs, by definition, can undergo osteogenesis.⁶ Recently, Lu et al. have demonstrated that preconditioning ASCs with tumor necrosis factor-alpha can further enhance this ability for the use of bone repair and regeneration.⁷⁸ It seems highly plausible that ASCs could be used to great effect in the regeneration of bone in dentistry, potentially reducing the need for second procedures, or even halting bone loss if caught early. Perhaps even more exciting are recent studies characterizing MSCs found in the dental pulp of molars, or dental pulp cells (DPSCs) which report full differentiation potential, with a greater osteo-dentinogenic potential.⁷⁹ These cells were also shown to be capable of regenerating the periodontium or become induced pluripotent stem cells,^{80,81} or even regenerate a dentin-pulp-like complex.⁸² These results offer promise for eventually replacing lost teeth without the use of current artificial procedures, and offer a relatively permanent solution.

References

1. Swan, M. Steady Advance of Stem Cell Therapies: Report from the 2011 World Stem Cell Summit, Pasadena, California, October 3–5. *Rejuvenation Res.* **14**, 699–704 (2011).
2. Gimble, J. M., Katz, A. J. & Bunnell, B. A. Adipose-derived stem cells for regenerative medicine. *Circ. Res.* **100**, 1249–1260 (2007).
3. Harasymiak-Krzyżanowska, I. *et al.* Adipose tissue-derived stem cells show considerable promise for regenerative medicine applications. *Cell. Mol. Biol. Lett.* 1–15 (2013). doi:10.2478/s11658-013-0101-4
4. Finer, N. Medical consequences of obesity. *Medicine (Baltimore)*. **39**, 18–23 (2011).
5. Katz, A. J., Lull, R., Hedrick, M. H. & Futrell, J. W. Emerging approaches to the tissue engineering of fat. *Clin. Plast. Surg.* **26**, 587–603, viii (1999).
6. Zuk, P. A. *et al.* Multilineage cells from human adipose tissue: implications for cell-based therapies. *Tissue Eng.* **7**, 211–228 (2001).
7. Amos, P. J. *et al.* IFATS collection: The role of human adipose-derived stromal cells in inflammatory microvascular remodeling and evidence of a perivascular phenotype. *Stem Cells* **26**, 2682–2690 (2008).
8. Amos, P. J. *et al.* Hypoxic culture and in vivo inflammatory environments affect the assumption of pericyte characteristics by human adipose and bone marrow progenitor cells. *AJP Cell Physiol.* **301**, C1378–C1388 (2011).
9. Natesan, S. *et al.* A bilayer construct controls adipose-derived stem cell differentiation into endothelial cells and pericytes without growth factor stimulation. *Tissue Eng. Part A* **17**, 941–953 (2011).
10. Rodbell, M. Metabolism of isolated fat cells. *J. Biol. Chem.* **241**, 130–139 (1966).
11. Cai, X., Lin, Y., Hauschka, P. V & Grottkau, B. E. Adipose stem cells originate from perivascular cells. *Biol. Cell* **103**, 435–447 (2011).
12. Liu, T. M. *et al.* Identification of common pathways mediating differentiation of bone marrow- and adipose tissue-derived human mesenchymal stem cells into three mesenchymal lineages. *Stem Cells* **25**, 750–760 (2007).

13. Yamada, Y., Wang, X. Di, Yokoyama, S. I., Fukuda, N. & Takakura, N. Cardiac progenitor cells in brown adipose tissue repaired damaged myocardium. *Biochem. Biophys. Res. Commun.* **342**, 662–670 (2006).
14. Cai, L. *et al.* IFATS collection: Human adipose tissue-derived stem cells induce angiogenesis and nerve sprouting following myocardial infarction, in conjunction with potent preservation of cardiac function. *Stem Cells* **27**, 230–237 (2009).
15. Salomone, F., Barbagallo, I., Puzzo, L., Piazza, C. & Li Volti, G. Efficacy of adipose tissue-mesenchymal stem cell transplantation in rats with acetaminophen liver injury. *Stem Cell Res.* **11**, 1037–1044 (2013).
16. Moshtagh, P. R., Emami, S. H. & Sharifi, A. M. Differentiation of human adipose-derived mesenchymal stem cell into insulin-producing cells: an in vitro study. *J. Physiol. Biochem.* (2012). doi:10.1007/s13105-012-0228-1
17. Okura, H. *et al.* Transdifferentiation of human adipose tissue-derived stromal cells into insulin-producing clusters. *J. Artif. Organs* **12**, 123–130 (2009).
18. Karaoz, E. *et al.* Adipose tissue-derived mesenchymal stromal cells efficiently differentiate into insulin-producing cells in pancreatic islet microenvironment both in vitro and in vivo. *Cytotherapy* **15**, 557–570 (2013).
19. Nambu, M. *et al.* Accelerated wound healing in healing-impaired db/db mice by autologous adipose tissue-derived stromal cells combined with atelocollagen matrix. *Ann. Plast. Surg.* **62**, 317–321 (2009).
20. Sacerdote, P. *et al.* Systemic administration of human adipose-derived stem cells reverts nociceptive hypersensitivity in an experimental model of neuropathy. *Stem Cells Dev.* **22**, 1252–63 (2013).
21. Bai, S. Autologous transplantation of adipose-derived mesenchymal stem cells ameliorates streptozotocin-induced diabetic nephropathy in rats by inhibiting oxidative stress, pro-inflammatory cytokines and the p38 MAPK signaling pathway. *Int. J. Mol. Med.* (2012). doi:10.3892/ijmm.2012.977
22. Mendel, T. a *et al.* Pericytes derived from adipose-derived stem cells protect against retinal vasculopathy. *PLoS One* **8**, e65691 (2013).
23. Rajashekhar, G. *et al.* Regenerative therapeutic potential of adipose stromal cells in early stage diabetic retinopathy. *PLoS One* **9**, e84671 (2014).
24. Yang, D. *et al.* The Relative Contribution of Paracrine Effect versus Direct Differentiation on Adipose-Derived Stem Cell Transplantation Mediated Cardiac Repair. *PLoS One* **8**, (2013).
25. Gneccchi, M., Zhang, Z., Ni, A. & Dzau, V. J. Paracrine mechanisms in adult stem cell signaling and therapy. *Circ. Res.* **103**, 1204–1219 (2008).

26. Traktuev, D. O. *et al.* A population of multipotent CD34-positive adipose stromal cells share pericyte and mesenchymal surface markers, reside in a periendothelial location, and stabilize endothelial networks. *Circ. Res.* **102**, 77–85 (2008).
27. Puissant, B. *et al.* Immunomodulatory effect of human adipose tissue-derived adult stem cells: comparison with bone marrow mesenchymal stem cells. *Br. J. Haematol.* **129**, 118–129 (2005).
28. Keats, E. C. & Khan, Z. A. Vascular stem cells in diabetic complications: evidence for a role in the pathogenesis and the therapeutic promise. *Cardiovasc. Diabetol.* **11**, 37 (2012).
29. Cianfarani, F. *et al.* Diabetes impairs adipose tissue-derived stem cell function and efficiency in promoting wound healing. *Wound Repair Regen.* 1–9 (2013). doi:10.1111/wrr.12051
30. Kim, H. K. *et al.* Alterations in the proangiogenic functions of adipose tissue-derived stromal cells isolated from diabetic rats. *Stem Cells Dev.* **17**, 669–680 (2008).
31. El-Ftesi, S., Chang, E. I., Longaker, M. T. & Gurtner, G. C. Aging and diabetes impair the neovascular potential of adipose-derived stromal cells. *Plast. Reconstr. Surg.* **123**, 475–485 (2009).
32. Cramer, C. *et al.* Persistent high glucose concentrations alter the regenerative potential of mesenchymal stem cells. *Stem Cells Dev.* **19**, 1875–1884 (2010).
33. Heng, L. Z. *et al.* Diabetic retinopathy: pathogenesis, clinical grading, management and future developments. *Diabet. Med.* **30**, 640–50 (2013).
34. Gardner, T. W., Antonetti, D. A., Barber, A. J., LaNoue, K. F. & Nakamura, M. New insights into the pathophysiology of diabetic retinopathy: potential cell-specific therapeutic targets. *Diabetes Technol. Ther.* **2**, 601–608 (2000).
35. Hammes, H.-P. *et al.* Pericytes and the pathogenesis of diabetic retinopathy. *Diabetes* **51**, 3107–3112 (2002).
36. Nguyen, Q. D. *et al.* Ranibizumab for diabetic macular edema: results from 2 phase III randomized trials: RISE and RIDE. *Ophthalmology* **119**, 789–801 (2012).
37. Han, Z., Guo, J., Conley, S. M. & Naash, M. I. Retinal Angiogenesis in the Ins2Akita Mouse Model of Diabetic Retinopathy. *Biochem. Mol. Biol.* **54**, 574–584 (2013).
38. Rakoczy, E. P. *et al.* Characterization of a mouse model of hyperglycemia and retinal neovascularization. *Am. J. Pathol.* **177**, 2659–2670 (2010).
39. Pollak, M. Insulin, insulin-like growth factors and neoplasia. *Best Pract. Res. Clin. Endocrinol. Metab.* **22**, 625–638 (2008).

40. Wang, Y. *et al.* Overexpression of osteopontin induces angiogenesis of endothelial progenitor cells via the $\alpha_v\beta_3$ /PI3K/AKT/eNOS/NO signaling pathway in glioma cells. *Eur. J. Cell Biol.* **90**, 642–648 (2011).
41. Deshmane, S. L., Kremlev, S., Amini, S. & Sawaya, B. E. Monocyte chemoattractant protein-1 (MCP-1): an overview. *J. Interferon Cytokine Res.* **29**, 313–326 (2009).
42. Jiang, X.-Y. *et al.* PGC-1 α prevents apoptosis in adipose-derived stem cells by reducing reactive oxygen species production in a diabetic microenvironment. *Diabetes Res. Clin. Pract.* 1–8 (2013). doi:10.1016/j.diabres.2013.03.036
43. Lai, C.-M. *et al.* Generation of transgenic mice with mild and severe retinal neovascularisation. *Br. J. Ophthalmol.* **89**, 911–916 (2005).
44. Takakura, N. *et al.* A role for hematopoietic stem cells in promoting angiogenesis. *Cell* **102**, 199–209 (2000).
45. Ebrahimian, T. G. *et al.* Cell therapy based on adipose tissue-derived stromal cells promotes physiological and pathological wound healing. *Arterioscler. Thromb. Vasc. Biol.* **29**, 503–510 (2009).
46. Mizuno, H. Adipose-derived stem cells for tissue repair and regeneration: ten years of research and a literature review. *J. Nippon Med. Sch. = Nihon Ika Daigaku zasshi* **76**, 56–66 (2009).
47. Chen, L., Tredget, E. E., Wu, P. Y. G. & Wu, Y. Paracrine factors of mesenchymal stem cells recruit macrophages and endothelial lineage cells and enhance wound healing. *PLoS One* **3**, e1886 (2008).
48. Wu, Y., Chen, L., Scott, P. G. & Tredget, E. E. Mesenchymal stem cells enhance wound healing through differentiation and angiogenesis. *Stem Cells* **25**, 2648–59 (2007).
49. Falanga, V. *et al.* Autologous bone marrow-derived cultured mesenchymal stem cells delivered in a fibrin spray accelerate healing in murine and human cutaneous wounds. *Tissue Eng.* **13**, 1299–1312 (2007).
50. Melero-Martin, J. M. *et al.* Engineering robust and functional vascular networks in vivo with human adult and cord blood-derived progenitor cells. *Circ. Res.* **103**, 194–202 (2008).
51. Ho, J. C. Y. *et al.* Reversal of endothelial progenitor cell dysfunction in patients with type 2 diabetes using a conditioned medium of human embryonic stem cell-derived endothelial cells. *Diabetes. Metab. Res. Rev.* **28**, 462–73 (2012).
52. Trudeau, K., Molina, A. J. A. & Roy, S. High Glucose Induces Mitochondrial Morphology and Metabolic Changes in Retinal Pericytes. *Invest. Ophthalmol. Vis. Sci.* **52**, 8657–8664 (2011).

53. Cooper, M. E. & El-Osta, A. Epigenetics: mechanisms and implications for diabetic complications. *Circ. Res.* **107**, 1403–1413 (2010).
54. Ling, C. & Groop, L. Epigenetics: a molecular link between environmental factors and type 2 diabetes. *Diabetes* **58**, 2718–2725 (2009).
55. Paneni, F., Costantino, S., Volpe, M., Lüscher, T. F. & Cosentino, F. Epigenetic signatures and vascular risk in type 2 diabetes: A clinical perspective. *Atherosclerosis* **230**, 191–7 (2013).
56. Prockop, D. J. & Youn Oh, J. Mesenchymal Stem/Stromal Cells (MSCs): Role as Guardians of Inflammation. *Mol. Ther.* **20**, 14–20 (2012).
57. Anton, K., Banerjee, D. & Glod, J. Macrophage-Associated Mesenchymal Stem Cells Assume an Activated, Migratory, Pro-Inflammatory Phenotype with Increased IL-6 and CXCL10 Secretion. *PLoS One* **7**, e35036 (2012).
58. Winkler, E. A., Bell, R. D. & Zlokovic, B. V. Central nervous system pericytes in health and disease. *Nat. Neurosci.* **14**, 1398–1405 (2011).
59. Hellström, M. *et al.* Lack of pericytes leads to endothelial hyperplasia and abnormal vascular morphogenesis. *J. Cell Biol.* **153**, 543–553 (2001).
60. Feng, J., Mantesso, A. & Sharpe, P. T. Perivascular cells as mesenchymal stem cells. *Expert Opin. Biol. Ther.* **10**, 1441–1451 (2010).
61. Loomans, C. J. M. *et al.* Endothelial progenitor cell dysfunction: a novel concept in the pathogenesis of vascular complications of type 1 diabetes. *Diabetes* **53**, 195–199 (2004).
62. Fadini, G. P. *et al.* Number and function of endothelial progenitor cells as a marker of severity for diabetic vasculopathy. *Arterioscler. Thromb. Vasc. Biol.* **26**, 2140–2146 (2006).
63. Tepper, O. M. *et al.* Human endothelial progenitor cells from type II diabetics exhibit impaired proliferation, adhesion, and incorporation into vascular structures. *Circulation* **106**, 2781–2786 (2002).
64. Beltramo, E. & Porta, M. Pericyte loss in diabetic retinopathy: mechanisms and consequences. *Curr. Med. Chem.* **20**, 3218–25 (2013).
65. Pfister, F. *et al.* Pericyte migration: a novel mechanism of pericyte loss in experimental diabetic retinopathy. *Diabetes* **57**, 2495–2502 (2008).
66. Caplan, A. I. All MSCs Are Pericytes? *Cell Stem Cell* **3**, 229–230 (2008).
67. Richardson, J. D. *et al.* Optimization of the Cardiovascular Therapeutic Properties of Mesenchymal Stromal/Stem Cells—Taking the Next Step. *Stem Cell Rev. Reports* (2012). doi:10.1007/s12015-012-9366-7

68. Herrmann, J. L. *et al.* Preconditioning mesenchymal stem cells with transforming growth factor-alpha improves mesenchymal stem cell-mediated cardioprotection. *Shock* **33**, 24–30 (2010).
69. Pasha, Z. *et al.* Preconditioning enhances cell survival and differentiation of stem cells during transplantation in infarcted myocardium. *Cardiovasc. Res.* **77**, 134–142 (2008).
70. Masoud, M. S. *et al.* Pre-conditioned mesenchymal stem cells ameliorate renal ischemic injury in rats by augmented survival and engraftment. *J. Transl. Med.* **10**, 243 (2012).
71. Hu, X. *et al.* Transplantation of hypoxia-preconditioned mesenchymal stem cells improves infarcted heart function via enhanced survival of implanted cells and angiogenesis. *J. Thorac. Cardiovasc. Surg.* **135**, 799–808 (2008).
72. Suzuki, K. *et al.* Heat shock treatment enhances graft cell survival in skeletal myoblast transplantation to the heart. *Circulation* **102**, III216–I221 (2000).
73. Rebelatto, C. K. *et al.* Expression of cardiac function genes in adult stem cells is increased by treatment with nitric oxide agents. *Biochem. Biophys. Res. Commun.* **378**, 456–461 (2009).
74. Mardas, N., Dereka, X., Donos, N. & Dard, M. Experimental Model for Bone Regeneration in Oral and Cranio-Maxillo-Facial Surgery. *J. Invest. Surg.* 1–18 (2013). doi:10.3109/08941939.2013.817628
75. Jensen, S. S. & Terheyden, H. Bone augmentation procedures in localized defects in the alveolar ridge: clinical results with different bone grafts and bone-substitute materials. *Int. J. Oral Maxillofac. Implants* **24 Suppl**, 218–236 (2009).
76. Esposito, M. *et al.* Interventions for replacing missing teeth: horizontal and vertical bone augmentation techniques for dental implant treatment. *Cochrane Database Syst. Rev.* CD003607 (2009). doi:10.1002/14651858.CD003607.pub3
77. Tonelli, P. *et al.* Bone regeneration in dentistry. *Clin. Cases Miner. Bone Metab.* **8**, 24–8 (2011).
78. Lu, Z. *et al.* Activation and promotion of adipose stem cells by tumour necrosis factor-alpha preconditioning for bone regeneration. *J. Cell. Physiol.* **228**, 1737–44 (2013).
79. Balic, A., Aguila, H. L., Caimano, M. J., Francone, V. P. & Mina, M. Characterization of stem and progenitor cells in the dental pulp of erupted and unerupted murine molars. *Bone* **46**, 1639–1651 (2010).
80. Lin, N.-H., Menicanin, D., Mrozik, K., Gronthos, S. & Bartold, P. M. Putative stem cells in regenerating human periodontium. *J. Periodontal Res.* **43**, 514–523 (2008).

81. Yan, X. *et al.* iPS cells reprogrammed from human mesenchymal-like stem/progenitor cells of dental tissue origin. *Stem Cells Dev.* **19**, 469–480 (2010).
82. Peng, L., Ye, L. & Zhou, X. Mesenchymal stem cells and tooth engineering. *Int. J. Oral Sci.* **1**, 6–12 (2009).

Appendix

Dead-cell Control Injection

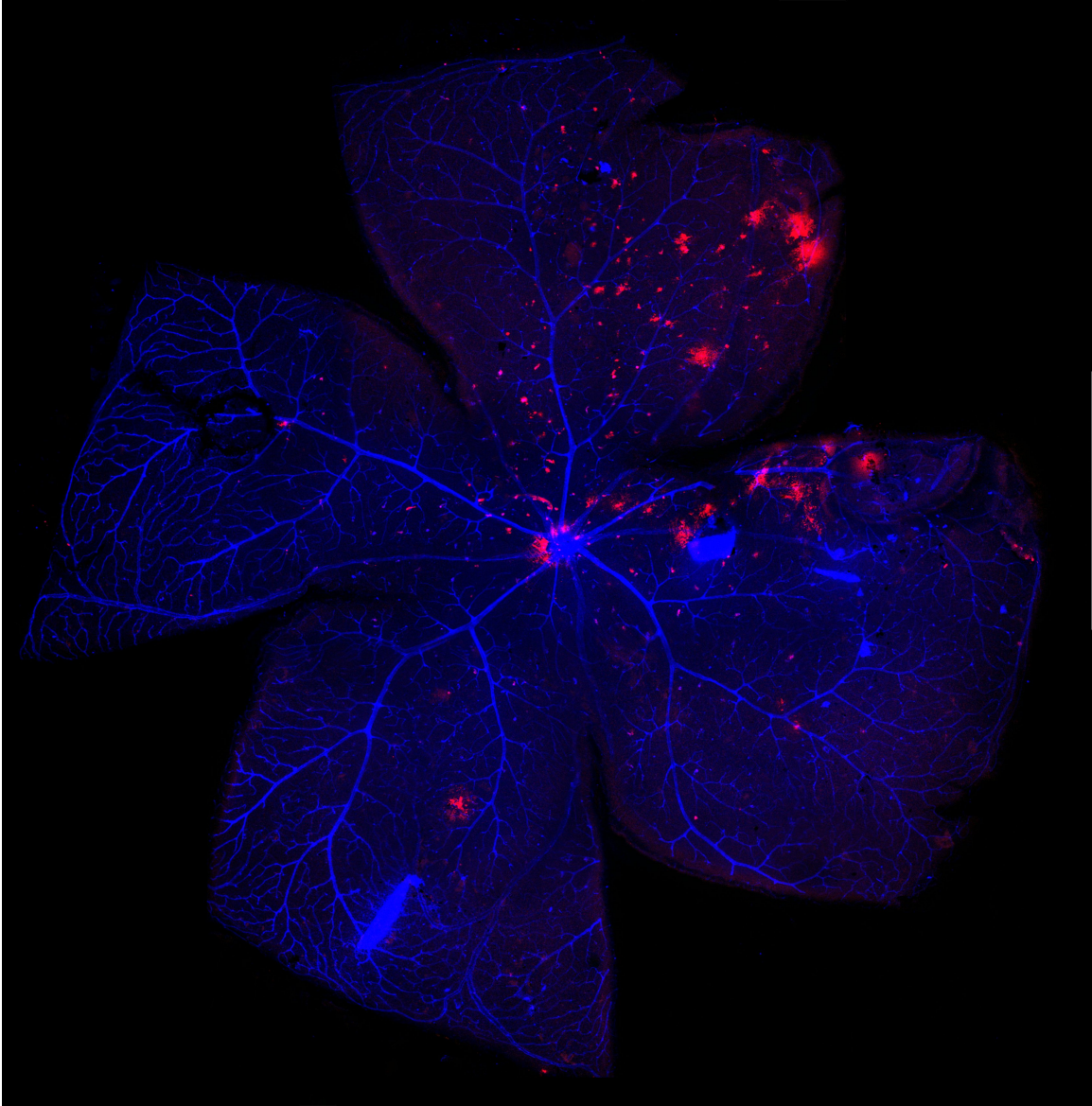
In addition to PBS contralateral controls, we also performed a treatment with dead cells to observe any effects in treatment not related to cell secretion or function, but merely due to the presence of cells/cell debris. Briefly, 5 week-old Akimba mice were injected with Dil-labeled and fixed mASCs. Fixation of mASCs was done by incubation with PFA for 10 minutes. At 9 weeks old, the treated retinae were harvested and stained for lectin. A representative retina can be seen in Appendix Figure A. A high amount of background in the lectin antibody binding and rapid photobleaching prevented any quantitative data from being generated from these retinae. It can be noted that the Dil-labeled, fixed cells do appear to persist in the retina, although any vascular protective effect is not readily apparent.

Akimba Retinae Pericyte Stain

To begin to ascertain whether injected mASCs were replacing lost pericytes, we stained untreated Akimba retinae for pericyte markers desmin and NG2. This was done for 5, 7, and 9 week-old Akimba mice. Retinae were harvested and stained in an identical manner to untreated mice. Appendix Figure B shows the results from this experiment. While there is a visually apparent decrease from 7 to 9 weeks of age, the large degree of variation in lectin and NG2 antibody binding makes obtaining useful results from these images problematic.

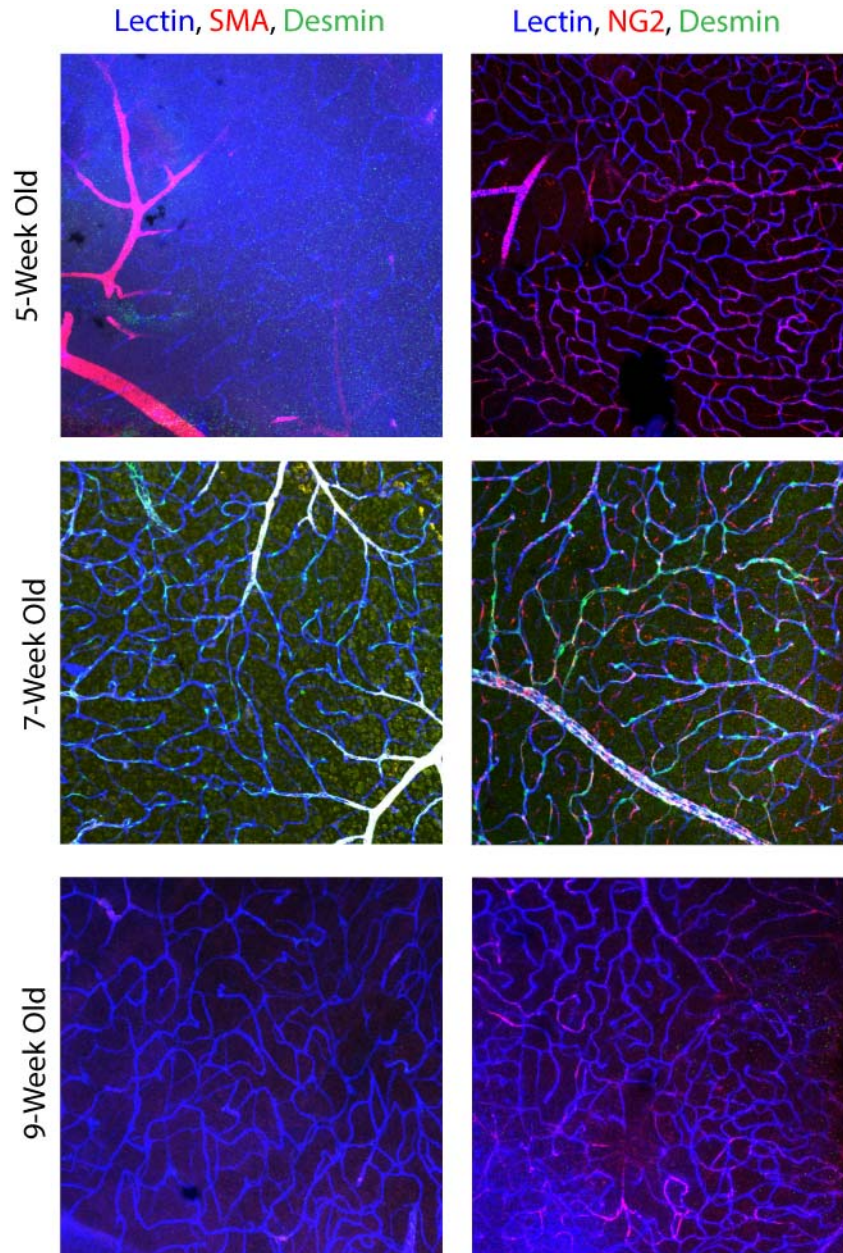
Appendix Figure A: Dead Cell-Injected Retina

Akimba eyes were injected with PFA-fixed/killed, Dil-labeled mASCs. Injection of dead cells, harvest of retinæ, and staining were performed in an identical manner to live cells described in Methods.



Appendix Figure B: Untreated Retinae, Stained for Pericyte Markers

Untreated Akimba retinae were harvested at a progression of time points (5 weeks old, 7 weeks, and 9 weeks) and stained for pericyte markers (desmin, NG2, and SMA) and lectin. Representative 20x confocal images are shown below.



Fair Use Checklist

Copyright Advisory Office
Columbia University Libraries
Kenneth D. Crews, Director
<http://copyright.columbia.edu>

Name: Stephen Cronk

Institution: University of Virginia

Project: M.S. Thesis - RE: Figures 4 & 5

Date: May 2014

Prepared by: _____

Purpose**Favoring Fair Use**

- ☐ Teaching (including multiple copies for classroom use)
- ☐ Research
- ☐ Scholarship
- ☐ Nonprofit educational institution
- ☐ Criticism
- ☐ Comment
- ☐ News reporting
- ☐ Transformative or productive use (changes the work for new utility)
- ☐ Restricted access (to students or other appropriate group)
- ☐ Parody

Opposing Fair Use

- ☐ Commercial activity
- ☐ Profiting from the use
- ☐ Entertainment
- ☐ Bad-faith behavior
- ☐ Denying credit to original author

Nature

Favoring Fair Use

- ☐ Published work
- ☐ Factual or nonfiction based
- ☐ Important to favored educational objectives

Opposing Fair Use

- ☐ Unpublished work
- ☐ Highly creative work (art, music, novels, films, plays)
- ☐ Fiction

Amount

Favoring Fair Use

- ☐ Small quantity
- ☐ Portion used is not central or significant to entire work
- ☐ Amount is appropriate for favored educational purpose

Opposing Fair Use

- ☐ Large portion or whole work used
- ☐ Portion used is central to or “heart of the work”

Effect

Favoring Fair Use

- ☐ User owns lawfully purchased or acquired copy of original work
- ☐ One or few copies made
- ☐ No significant effect on the market or potential market for copyrighted work
- ☐ No similar product marketed by the copyright holder
- ☐ Lack of licensing mechanism

Opposing Fair Use

- ☐ Could replace sale of copyrighted work
- ☐ Significantly impairs market or potential market for copyrighted work or derivative
- ☐ Reasonably available licensing mechanism for use of the copyrighted work
- ☐ Affordable permission available for using work
- ☐ Numerous copies made
- ☐ You made it accessible on the Web or in other public forum
- ☐ Repeated or long-term use